2008

NMR Analyses Show TCDD Elicits Differences in Hepatic Metabolism in Female C57BL/6 Mice and Sprague-Dawley Rats

Meghan Katherine Makley
Wright State University

NMR ANALYSES SHOW TCDD ELICITS DIFFERENCES IN HEPATIC METABOLISM IN FEMALE C57BL/6 MICE AND SPRAGUE-DAWLEY RATS

A thesis submitted in partial fulfillment
of the requirements for the degree of
Master of Science

By

MEGHAN KATHERINE MAKLEY
B.S. University of Dayton, 2004

2008
Wright State University

WRIGHT STATE UNIVERSITY

SCHOOL OF GRADUATE STUDIES

Date of defense: 12-11-08

I HEREBY RECOMMEND THAT THE THESIS PREPARED UNDER MY SUPERVISION BY Meghan Katherine Makley ENTITLED NMR Analyses Show TCDD Elicits Differences in Hepatic Metabolism in Female C57BL/6 Mice and Sprague-Dawley Rats BE ACCEPTED IN PARTIAL FULFILLMENT OF THE REQUIREMENTS FOR THE DEGREE OF Master of Science.

_____
Nicholas V. Reo, Ph.D.
Thesis Director

_____
Steven J. Berberich, Ph.D.
Department Chair

Committee on Final Examination

_____
Nicholas V. Reo, Ph.D.

_____
Darrell E. Fleischman, Ph.D.

_____
Lawrence J. Prochaska, Ph.D.

_____
Joseph F. Thomas, Jr., Ph.D.
Dean, School of Graduate Studies

ABSTRACT

Makley, Meghan Katherine. M.S., Department of Biochemistry and Molecular Biology, Wright State University, 2009.
NMR Analyses Show TCDD Elicits Differences in Hepatic Metabolism in Female C57BL/6 Mice and Sprague-Dawley Rats.

TCDD (2,3,7,8-tetrachlorodibenzo-*p*-dioxin) elicits tissue-, sex-, and species-specific effects. This study compares the hepatic response to an oral dose of TCDD in immature ovariectomized (i.o.) C57BL/6 mice (30 μg/kg) and i.o. Sprague-Dawley rats (10 μg/kg), at 72, 120, and 168 h post-dose. Hepatic lipid extracts were analyzed by ^{13}C and ^{31}P NMR, and aqueous extracts by ^{1}H and ^{31}P NMR.

Consistent with increased lipid content in mice ($p \leq 0.05$), TCDD induced increases in hepatic triacylglycerides (TAG), cholesterol, and fatty acids. Principal component analysis of ^{13}C spectra show treatment groups separate in mice, but not rats. Mice showed decreases in the lactate/pyruvate ratio and dihydroxyacetone phosphate, consistent with decreased cytosolic NADH/NAD^+ ratio and upregulated TAG synthesis. TCDD-treated rats exhibited decreased levels of sphingomyelin, and three-fold increase in phosphocholine, suggesting TCDD activates sphingomyelinase. Both species showed similar decreases in cardiolipin, indicating oxidative stress. These observations are compared with hepatic histopathology and gene expression findings.

TABLE OF CONTENTS

LIST OF FIGURES

LIST OF TABLES

I. INTRODUCTION

The aryl hydrocarbon receptor (AhR) is a cytosolic ligand-activated member of the basic-helix-loop-helix Per (Period)-ARNT (aryl hydrocarbon nuclear translocator)-SIM (single-minded) (bHLH-PAS) domain superfamily of proteins. This family of proteins mediates the toxic effects of halogenated aromatic hydrocarbons. Halogenated aromatic hydrocarbons are a group of widespread, persistent, and toxic environmental contaminants that include the polychlorinated dibenzo-*p*-dioxins, dibenzo-furans, and biphenols (Schecter *et al.*, 2006). The structure of 2,3,7,8-tetrachlorodibenzo-*p*-dioxin (TCDD, dioxin) consists of two benzene rings connected by two oxygen atoms and contains four chlorines. TCDD has a long half-life. In humans, it is seven to eleven years (Pirkle *et al.*, 1989), and in rodents, it is two to four weeks (Rose *et al.*, 1976).

These compounds are formed during the production of halogen-containing aromatics, such as herbicides (Agent Orange) during the Vietnam War, and during the combustion of dust or bleaching of pulp at paper mills. Cases of TCDD exposure occur via industrial accidents, occupational exposure, or environmental pollution, such as volcanic emissions. Another well-known instance was in 1976, when a trichlorophenol manufacturing plant exploded in Seveso, Italy.

Type-2 diabetes has been associated with TCDD exposure among Vietnam veterans exposed to Agent Orange (Fujiyoshi *et al*., 2006), those exposed to TCDD in Seveso, Italy (Bertazzi *et al.*, 1998), and other industrial workers (Vena *et al*., 1998).

People with high levels of TCDD demonstrate insulin resistance (Cranmer *et al*., 2000).

TCDD induces a broad spectrum of additional effects such as the induction of metabolizing enzymes (cytochrome-P450), cancer, immunotoxicity, hepatotoxicity, endocrine disturbances, and wasting syndrome. The wasting syndrome is a failure to gain weight at normal rates, or in more severe cases, weight loss. Non-alcoholic fatty liver disease, the metabolic syndrome, and obesity are also linked to TCDD.

Interestingly, TCDD causes different phenotypic responses in different species and even in different strains of some species. There is a wide range of lethal doses (LD_{50}s) in rodents. Guinea pigs are very sensitive to TCDD (LD_{50} = 1 μg/kg) and hamsters are among the most resistant (LD_{50} = 1000 μg/kg). The species used in this study, C57BL/6 mice and Sprague Dawley rats, have LD_{50}s of 120 μg/kg and 30 μg/kg, respectively (Bickel 1982; Vos *et al*., 1974).

Classic rodent responses that are observed include effects on liver and body weight gain (Poland and Knutson, 1982). One study, using these same strains, reported that liver weights of both TCDD-treated rats and mice significantly increased compared to vehicle controls after 72 and 168 hours ($p<0.05$). In rats, body weight gain significantly decreased compared to controls at 72 and 168 hours. Mice showed no significant alterations in body weight or body weight gain (Boverhof *et al.*, 2006).

Histochemical findings in both species were reported in this same study (Boverhof *et al*., 2006). TCDD-treated rats exhibit minimal to moderate hepatocellular hypertrophy in the centriacinar regions of the liver. Such hypertrophy included enlarged hepatocytes, and a more granular, eosinophilic and less vacuolated cytoplasm compared to controls. In TCDD-treated mice, vacuolization was first observed in the periportal and

midzonal regions, and then the centriacinar regions. Also, vacuolization was progressive from 72 to 168 hours, at which point cell apoptosis occurred. Oil Red O staining confirmed that this vacuolization was due to lipid accumulation, and this was observed in mouse but not rat liver.

The mechanisms of toxicity in rats and mice are not understood, but likely deal with the AhR signaling pathway. Most of TCDD's effects require activation of the AhR, which results in transcriptional induction or repression of genes (Puga *et al*., 2000), including those of the Ah gene battery (Hankinson *et al.*, 1991; Hankinson 1995; Kafafi *et al*., 1993; Nebert 1989; Nebert *et al*., 1993, 2000). The AhR-binding affinity for TCDD is similar between rats and mice, so it cannot explain the difference in sensitivity (Denison *et al*., 1986; Poland *et al*., 1976). The rat and mouse AhR are comparable but not identical molecular species and differ in molecular weights (Denison *et al*., 1986). There is high homology in the amino acid sequences except in a 42-amino acid truncation at the C-terminal end of mouse AhR when compared to rat. Therefore, differences in the AhR transactivation domain may explain differential gene expression responses and altered sensitivity of these strains. However, this was reported for Han/Wistar and Long-Evans rats (Okey *et al*., 2005), strains not used in this study. Differences in genomic sequences at promoter and enhancer regions are an alternative explanation for the species differences (Sun *et al*., 2004).

The mechanisms of toxicity are also believed to be related to estrogen receptors (ER), endocrine disruptors, and estradiol, so immature ovariectomized (i.o.) female rodents were used. Other groups found that the mechanisms of toxicity are estrogen-dependent in rat liver (Lucier *et al*., 1991; Sewall *et al*., 1993). In rats, females appear

more sensitive to liver carcinogenicity of TCDD. Ovariectomy inhibited the promotion of TCDD-induced preneoplastic foci and liver tumors; hence, ovarian hormones are believed to play a role (Lucier *et al.*, 1991). Petroff and coworkers found that estrogen amplified TCDD-induced changes in body weight and hepatic cytochrome-P450 enzyme induction (Petroff *et al.*, 2001). Kociba and coworkers found that dietary administration of TCDD for two years to Sprague Dawley rats induces liver tumor formation in females, but not males, and this response seems to be linked to hormone expression (Kociba *et al*., 1978).

The AhR also appears to be linked to endocrine disruptors as well as estrogen. The AhR and ARNT are present in mammary tissues, and inactivation of these proteins results in impaired mammary development and lactation (Abbott *et al*., 1999; Birnbaum and Fenton 2003; Hushka *et al*., 1998; Le Provost *et al*., 2002; Warner *et al*., 2002). Vorderstrasse and coworkers reported that AhR activation during pregnancy disrupts mammary gland differentiation (Vorderstrasse *et al*., 2004). Mammary tissue may be susceptible to injury by endocrine disruptors. Also, TCDD and AhR modulators can activate inhibitory AhR-ER-α crosstalk in the uterus and breast and endometrial cancer cells (Safe 2001).

This study uses NMR-based quantitative metabolomics to compare hepatic effects of TCDD in rats and mice. Three genomic studies reveal genes or mRNA expression that are 1) regulated by the AhR or 2) altered after TCDD administration in vivo. Zacharewski and coworkers investigated TCDD-induced temporal changes in hepatic gene expression and serum clinical chemistry, and proposed a mechanism of hepatotoxicity in mice (Boverhof *et al*., 2005). They identified genes uniquely up- or

downregulated in mice and rats, as well as conserved responses (Boverhof *et al*., 2006). Fletcher and coworkers studied mRNA expression in liver; however, they used male Sprague-Dawley rats after a single administration of 40 μg TCDD/kg body weight (Fletcher *et al*., 2005). One must be careful when making comparisons to i.o. female rats. The metabolic pathways differently affected by TCDD in mice and rats were identified using the metabolic data presented here, and then compared with these mRNA and gene expression findings.

II. MATERIALS AND METHODS

A. MATERIALS

Chemicals: Methanol and chloroform came from Fisher-Scientific; deuterium oxide (D_2O), deuterchloroform ($CDCl_3$), trimethylsilyl-3-propionic acid sodium salt (TSP), ethylenediaminetetraacetic acid (EDTA), and methylenediphosphonic acid (MDPA) from Sigma-Aldrich (St. Louis, MO); Chelex 100 from BIORAD, and liquid nitrogen from Weiler Welding (Dayton, OH).

Animals: Female Sprague Dawley rats and C57BL/6 mice came from Charles River Laboratories (Raleigh, NC).

NMR Spectroscopy Analysis: Varian NMR (VNMR) version 6.1 computer system came from Varian Inc. (Houston, TX); JMP statistical software from SAS (Cary, NC); and Chenomx NMR suite version 5.0 profiler and processor (Edmonton, Alberta).

B. METHODS

Animal Protocol

Female Sprague Dawley rats and C57BL/6 mice, ovariectomized by the vendor on post-natal day (PND) 20 and all having body weights within 10% of the average body weight, were obtained from Charles River Laboratories (Raleigh, NC) on PND 25. This model has been previously used to investigate the effects of TCDD (Boverhof *et al*., 2005, 2006) on clinical chemistry, hepatic gene expression, and histopathology. It was used in the present study to obtain metabolomic data elucidate the mechanisms associated

with TCDD-elicited hepatotoxicity. Animals were housed in polycarbonate cages containing cellulose fiber chips (Aspen Chip Laboratory Bedding, Northeastern Products, Warrensberg, NY) in a 23 °C high-efficiency particulate air-filtered environment with 30-40% humidity and a 12-hour light/dark cycle (0700-1900 hours). Animals were allowed free access to deionized water and Harlan Teklad 22/5 Rodent Diet 8640 (Madison, WI), and acclimatized for four days prior to dosing. On the fourth day, animals were weighed, and a stock solution of TCDD (provided by S. Safe, Texas A&M University, College Station, TX) was diluted in sesame oil (Sigma, St. Louis, MO) to achieve the desired dose based on the average weight. Doses were chosen to elicit moderate hepatotoxicity without overt toxicity and were based upon cytochrome-P450 enzyme (CYP1A1) induction. C57BL/6 mice were treated with either 0.1 mL of sesame oil (vehicle control, n=5) or 30 μg/kg TCDD in sesame oil (treated, n=5) by oral gavage. Sprague Dawley rats were treated with 0.1 mL of sesame oil or 10 μg/kg TCDD (n=5 per group), also by oral gavage.

At 72, 120, or 168 hours post-dose, animals were sacrificed by cervical dislocation, and livers were removed, weighed, and frozen in liquid nitrogen. Animal work was done at Michigan State University, with the approval of its All-University Committee on Animal Use and Care. Livers (*ca*. 0.5 g) were shipped overnight on dry ice to Wright State University (Cox Institute) in Dayton, Ohio for extractions and NMR spectroscopy analyses.

Dual-Phase Extraction Procedure

A three-day dual-phase extraction procedure yielded aqueous and lipid extracts from *ca*. 0.5 g of liver. On day one, individual livers were crudely pulverized under

liquid nitrogen with mortar and pestle and then weighed. Ground livers were homogenized in 0.7 mL/100 mg liver in a 1:1:1 volume of methanol, chloroform, and water using a glass tissue grinder with a Teflon pestle. The homogenate was allowed to sit in an ice bath for fifteen minutes. The mixture was transferred to a 50 mL glass centrifuge tube and spun at 2000 x g for 25 minutes at 4 °C. The sample was transferred through filter paper (pre-washed with 0.5 mL each of water, chloroform, and methanol) into a separatory funnel (set in a refrigerator at 4 °C). The pellet was washed three times with 0.5 mL each of water, chloroform, and methanol. After each wash, the pellet was homogenized, left in an ice bath for five minutes, and centrifuged for five minutes. The supernatant was then transferred to the separatory funnel. The separatory funnel was left at 4 °C for 17-24 hours to allow complete separation of the two phases.

On day two, the upper phase (aqueous constituents) was drawn off using a disposable pipette into a clear vial. The lower, organic phase (lipids) was removed to an amber vial and evaporated to dryness using a gentle stream of nitrogen gas. The funnel was washed three times with 0.5 mL each of water, chloroform, and methanol. The aqueous phase was partially evaporated under nitrogen gas to remove most of the methanol, and then lyophilized to dryness overnight. The lipid extract was placed under mild vacuum overnight to ensure complete dryness. On day three, each vial was weighed to obtain total content. The lipids were reconstituted in $CDCl_3$, and then both vials were stored at -20 °C.

NMR Spectroscopy of Liver Extracts

Sample preparation for NMR spectroscopy acquisition differed for lipid and aqueous extracts, and is described in their respective sections below. All samples, after

reconstitution, were placed in a 5-mm NMR tube. All NMR spectra were acquired using a Varian INOVA spectrometer at 14.1 T. ^{13}C, ^{31}P, ^{1}H NMR spectroscopy were performed at 150, 243, and at 600 MHz, respectively. All data were acquired in field-lock mode using the deuterium signal from $CDCl_3$.

1. NMR Spectroscopy of Lipid Extracts

Lipid samples were reconstituted in 600 μL D_2O with 1.04 mM TSP in D_2O added as a chemical shift reference at 0.0 ppm. 500 μL of this reconstituted sample were added to the NMR tube. Quantitative ^{13}C and ^{31}P NMR spectroscopy were performed on the hepatic lipid extracts. High resolution proton-decoupled ^{31}P and ^{13}C NMR spectra were acquired in field-lock mode using a 5-mm probe operating at 242.8 and 150.8 MHz, respectively. The sample temperature was regulated at 20 °C in order to obtain optimal spectral resolution (Adinehzadeh *et al*., 1998). ^{13}C and ^{31}P lipid samples were acquired with the Nuclear Overhauser Effect (NOE) using a gated ^{1}H-decoupling sequence. Data acquisition parameters for ^{31}P included a 90 ° pulse, 645 Hz spectral bandwidth, 1.6 second acquisition time, 10.6 second interpulse delay (full T_1 relaxation) and *ca.* 2.25 hours of signal averaging. ^{13}C samples were acquired using a 70 ° pulse, 35 kHz spectral bandwidth, 1.3 second acquisition time, 1.9 second interpulse delay and *ca.* 15 hours of signaling averaging.

Preparation of Cs_2EDTA Salt

For the ^{31}P NMR, a 90 mM Cs_2EDTA solution was made to help improve the signal to noise resolution. A 1 M solution of EDTA free acid was made in a total volume of 3 mL, as well as a 0.6 M CsOH solution in a total volume of 15 mL. The EDTA solution was titrated with the CsOH solution to pH 6.0, using *ca.* 10 mL of CsOH. The

solution was frozen and lyophilized to dryness. During the preparation of this 90 mM Cs_2EDTA solution, crystals were dissolved in 1 mL distilled deionized water, to which 4 mL of methanol were added (Meneses *et al*., 1988). To the NMR tube, 200 µL of this Cs_2EDTA solution were added. The solution was agitated, and the tube was allowed 45 minutes for separation. In some cases, an additional 25 µL of Cs_2EDTA needed to be added to improve the signal to noise resolution of certain phospholipids. The ^{31}P NMR spectroscopy was run after the ^{13}C.

2. NMR Spectroscopy of Aqueous Extracts

Dried aqueous extracts were treated with Chelex 100 and 2 mL water to remove divalent cations, and then lyophilized to dryness again. Samples were reconstituted in 750 µL of 1.04 mM TSP in D_2O, 650 of this volume transferred to an NMR tube for the ^1H NMR spectroscopy. Aqueous samples were run at 25 °C. After the ^1H NMR was finished, 50 µL of a 2:1 mix of Na_2EDTA (215 mM) to MDPA (84.7 mM) solution was added for ^{31}P NMR spectroscopy. The ^1H decoupler was used only when running the ^{31}P NMR spectroscopy.

Spectral Data Analysis

All spectral processing was done on a Sun Microsystems computer using VNMR version 6.1 software (Varian Inc. Houston, TX) that utilized exponential multiplication yielding 0.3, 0.5, and 1 Hz line-broadening, for ^1H, ^{13}C, and ^{31}P, respectively. The first step was to perform weighted Fourier transformation of the free induction decay, or FID. Then, the spectrum was phased and baseline corrected. For the lipid extracts, the reference was set to the center peak of $CDCl_3$ at 77.79 ppm for ^{13}C NMR spectra and to phosphatidylcholine (PtdC) at -0.84 ppm for ^{31}P NMR spectra; and for the aqueous

extracts, to TSP at 0.0 ppm for ^{1}H NMR spectra and to glycerophosphocholine (GPC) at 3.082 ppm for ^{31}P NMR spectra. GPC was chosen relative to phosphocreatine at 0.0 ppm; however, the liver does not contain phosphocreatine. The chemical shift of GPC is not pH-sensitive.

^{31}P NMR spectra of lipids were fit by Lorentizian line-shape analysis (due to simplicity). All peaks of interest were thresholded, deconvoluted, and then integrated. Metabolites were quantified based on the PtdC integral.

Several samples had to be spiked in order to verify the chemical shift assignment of several metabolites. This was necessary because of slight differences in pH from sample to sample, since many phosphorus signals are pH dependent. Our liver extracts are believed to be at pH 7-8. Spiking was done by adding a small amount of the metabolite to an old liver sample, and running NMR spectroscopy. The spectrum with the spiked sample was compared to the original spectrum of that sample (used for processing, quantification, etc.) to determine which peak that metabolite represented. A general flowchart of the entire experimental protocol can be seen in Appendix B.

Data Processing for PCA

^{13}C NMR spectra were divided into 1024 bins and ^{1}H NMR spectra into 280 bins. Principal Component Analysis (PCA) was performed, to characterize changes in the lipid profiles in each species. PCA reduces multidimensional data sets to lower dimensions for analysis, and looks for patterns (pattern recognition analysis). It is an unsupervised method, in that it does not know which data set is treated or control, etc (Jahns *et al*., 2008). After PCA was performed, the signals of metabolites of interest were quantified. Peak integrals were quantified relative to the known concentration of $CDCl_3$ solvent in

the NMR tubes, after correction for T_1 saturation. Data were normalized to the total lipid weight per gram of liver.

All ^1H spectra were analyzed using a website developed by a bioinformatics research group at Wright State (http://birg.cs.wright.edu/cox/user_login/login). The xy files are loaded to the website, and a new analysis is created, to which collections of spectra can be added. The operations are performed on these spectral groups. Spectra were cropped to start at 11.6 ppm. Then, the threshold range was set to {11.6, 10.0; -0.18, -2}. The number of standard deviations was set to three, and the number of spikes to four. Then, the spectrum was cropped to 10 to 0.18 ppm to mark the water region for deletion. The region at 5.09 to 4.58 was zeroed. This region also includes the glucose doublet, as this varied across animals due to interference from the water signal. After the processing step, PCA was then run, and then the *t*-test, bin-by-bin, to evaluate control *vs.* treated differences at each time-point. Then, the Orthogonal Partial Least Squares Discriminant Analysis (OPLS-DA) test was performed.

Quantification

In order to do the quantification on a μmol/g liver basis, the final volume in the NMR tube needs to be obtained. This was done by adding the volume of sample transferred to the NMR tube and the volume of 1:2 MDPA:EDTA solution added to the NMR tube.

The next step was to determine the concentration of $CDCl_3$ in the NMR tube. This could be obtained, knowing the concentration of the stock that was made.

In the case of the ^{31}P NMR spectra of aqueous extracts, the intensity of MDPA started out at 100, but needed to be corrected for the number of equivalent phosphorus, of which MDPA has two. Here, the corrected intensity of MDPA is 50.

For the quantification of lipids, the volume of the organic phase was corrected, taking into consideration the temperature of the lab and density. Adding some amount of distilled water to an NMR tube, the tube was weighed and the height of the water measured. The volume was calculated from 1) its density and weight, and 2) the volume of the cylinder or tube. The ratio of the true volume to calculated volume was obtained. The procedure was repeated three times, and the average and standard error obtained.

The change in volume factor was found to be 0.355. The final volume in the NMR tube of the $CDCl_3$ phase was found to be 0.571, based on the volume of the sample transferred to the tube added to 0.355 multiplied by the volume of Cs_2EDTA.

After inputting the intensities for each animal, the intensity was divided by the number of equivalent carbons represented in the spectrum. The intensity ratio measured, would be derived by taking the intensity and dividing that by that of MDPA, or 50. Then the intensity ratio (corrected for T_1 saturation and the NOE), is determined. This correction involved acquiring data under fully relaxed (FR) acquisition conditions for a representative sample (5 T_1's without NOE; interpulse delay of 250 s). The ratio of the intensity of a peak of interest to the intensity of $CDCl_3$ (quantification standard) was then calculated for FR and partially saturated (PS) spectra. Saturation factors (SFs) were then determined by calculating the ratio of FR to PS intensities for each peak of interest. This ratio was normalized to the intensity of the metabolite peak and to the solvent $CDCl_3$.

Now the concentration of the metabolite in the NMR tube can be obtained, which

would be the concentration of MDPA in the tube, multiplied by the intensity ratio that has been corrected for T_1 saturation. This number is then multiplied by the final volume in the tube divided by the volume of sample transferred to the NMR tube to obtain the concentration of that metabolite in the reconstituted sample, also in mM. This number is multiplied by the volume of D_2O used for sample reconstitution to get the quantity of your metabolite in μmol, and then this μmol number is divided by the number of grams of liver in the sample to get μmol/g liver.

The concentration of PtdC from the ^{13}C spectrum was obtained based on the concentration of $CDCl_3$, and was used to quantify all the phospholipids, on a μmol/g of liver basis. See Appendix C for sample calculations.

^{1}H NMR Spectroscopy of Aqueous Extracts

Chenomx NMR suite (version 5.0) profiler and processor were used to determine the concentration of lactate (in mM) in the ^1H aqueous NMR sample. Line-broadening of 0.3, phasing, and linear baseline correction were performed. The water region was also deleted.

Statistical Analysis

Statistical analyses involving more than two groups utilized an analysis of variance (ANOVA). The three-factor ANOVA or multifactor test was used to assess significant differences among species (mouse *vs*. rat), treatment (control *vs*. treated), and time (72, 120, and 168 hours). If the p-value was less than or equal to 0.05, the data were considered statistically significant. However, if the three-factor ANOVA was not significant ($p>0.05$), the two-factor ANOVA was performed, evaluating the effects on treatment and time, time and species, or treatment and species. If the two-factor ANOVA

proved not significant, the one-factor ANOVA was then used, to assess significant differences among treatment groups or across time. For each significant effect of treatment, the Fisher least squares means (LSM) and Tukey honestly significant differences (HSD) tests were used for comparison of multiple group means. The Student's *t*-test was used to determine the effects of TCDD across treatment at each time post-dose, or across time with each treatment. Error estimates are given as standard error of the mean (SE), and *n*-values are given in the legends to figures. See Appendix D for a flowchart of the ANOVA tests.

III. RESULTS

NMR spectroscopy of the lipid and aqueous phases of the liver extracts was used to identify significant quantitative changes in metabolites between control and treated groups, mice and rats, and over time post-dose with TCDD. Also examined were the hepatic lipid and aqueous content per gram of liver. Results from the hepatic lipid and aqueous extracts are discussed below in their respective sections.

A. LIPID EXTRACTS

1. Effects of TCDD on Mean Total Hepatic Lipid Content

Figure 1 shows the mean liver lipid content (mg lipid/g liver) in TCDD-treated and vehicle control animals (mice and rats) at 72, 120, and 168 hours post-dose. A three-factor ANOVA was conducted using species (mouse and rat), treatment groups (treated and control), and time (72, 120, and 168 hours) as factors. The three-factor ANOVA shows that the data in the whole model of mean lipid content is significant ($p=0.0014$). This whole model analysis indicates that significant differences occur between species and treatment groups ($p=0.0128$), but not across time. Treated *vs*. control mice show the largest differences, with mean liver lipid content 34-55% greater in treated mice relative to controls across time. Treated *vs*. control rats do not show significant differences.

The one-factor ANOVA was also conducted, within each species, to examine significant differences across time (72, 120, and 168 hours) or between treatment groups (treated *vs*. control). In mice, mean lipid content in treated animals is significantly higher

relative to controls at 72 (p=0.0037) and 168 (p=0.0476) but not 120 hours. Mean lipid content is not significantly changed between TCDD-treated and control rats, at any time post-dose. There are no statistical differences across time in either species. This may be explained by the great variability in treated mice at 120 hours. These findings indicate that TCDD causes steatosis, or fatty liver, in mice but not rats.

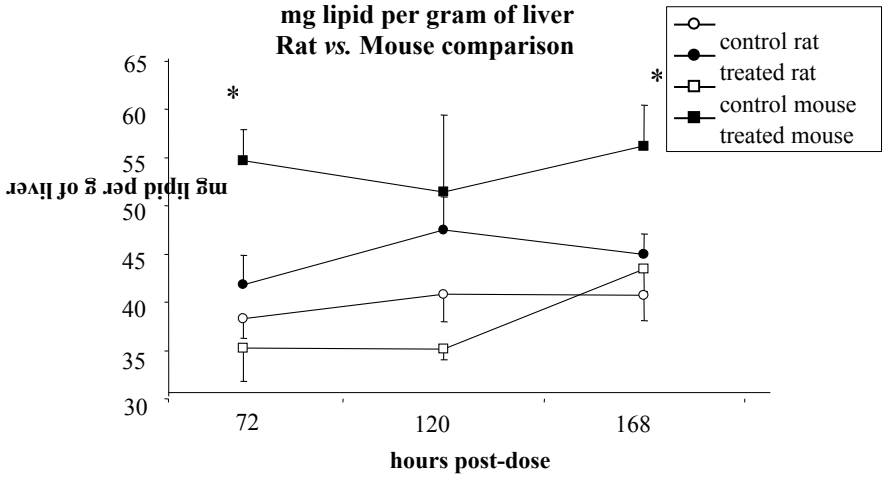

FIG. 1. Species comparison of mean lipid weights per gram of liver as a function of time post-dose. The legend shows symbols for rat and mouse control and treatment groups. Effects were examined at 72, 120, and 168 hours post-dose. The asterisk denotes a significant difference in treated *vs*. control mice at the specified time ($p \leq 0.05$). See Table 2 for statistical differences across time.

Summary of Mean Total Hepatic Lipid Content

To facilitate comparison between mouse and rat, mean hepatic lipid content (mg lipid/g liver) for control and treated animals (mice and rats) at each of the three times post-dose are summarized in Table 1. Also indicated are statistical differences between control and treated animals at the indicated time post-dose. A separate table shows the statistical differences using the three-factor ANOVA, including time effects (Table 2).

TABLE 1. Mean hepatic lipid content in TCDD-treated and vehicle control mice and rats at 72, 120, and 168 h post-dose (Mean ± SE; mg lipid/g liver; *n*=4-5 per group). The asterisk denotes significant differences ($p \leq 0.05$) between TCDD-treated and vehicle control animals at the specified time post-dose (one-factor ANOVA with post-hoc Tukey-Kramer HSD). C=control, T=treated, h=hour.

	Mouse					
	72 h		120 h		168 h	
	C	T	C	T	C	T
Lipid Content (mg lipid/g liver)	35.3 ± 3.50	54.7 ± 3.26*	38.4 ± 1.09	51.5 ± 7.95	40.6 ± 2.37	56.2 ± 4.28*

TABLE 2. Effect-derived differences in mean hepatic lipid content (mg lipid/g liver) for treatment, species, and time. Statistical significance was determined by a three-factor ANOVA testing effect across species, treatment, and time, with JMP statistical software (SAS, Cary, NC, US). If the whole model ANOVA was significant ($p \leq 0.05$), then appropriate LSM Differences, HSD, or LSM Differences Student's *t*-test was performed. Treatment effect shows differences between all animals independent of species, and then within each species (mouse or rat) due to treatment. Species effect shows differences between all animals independent of treatment, then within treatment groups (treated or control), based on species. Time effect shows differences between the three time-points, between all animals, and then by species. See Appendix for flowchart of ANOVA tests. M=mouse, R=rat, T=treated, C=control, h=hour post-dose, NS=no significant difference detected, NA=not appropriate. The p-values are not adjusted for multiple testing.

Treatment (treated *vs.* control)			**Species (mouse *vs.* rat)**			**Time (72 h *vs.* 120 h *vs.* 168 h)**		
Main Effect (M + R)	**M**	**R**	**Main Effect (T + C)**	**T**	**C**	**Main Effect (M + R)**	**M**	**R**
NA	T > C 34-55% (p=0.0128)	NS	NA	M > R 8-31% (p=0.0128)	NS	NS	NS	NS

2. PCA for Hepatic Lipids in Mice and Rats Analyzed by ^{13}C NMR Spectroscopy

PCA was performed on the combined datasets of mice and rats, and in Figure 2, the data separated into three groups: 1) control mice, 2) treated mice, and 3) control and treated rats. There appears to be one outlier: a control mouse sample, indicated by the arrow. Again, this suggests that TCDD causes steatosis in mice and not rats.

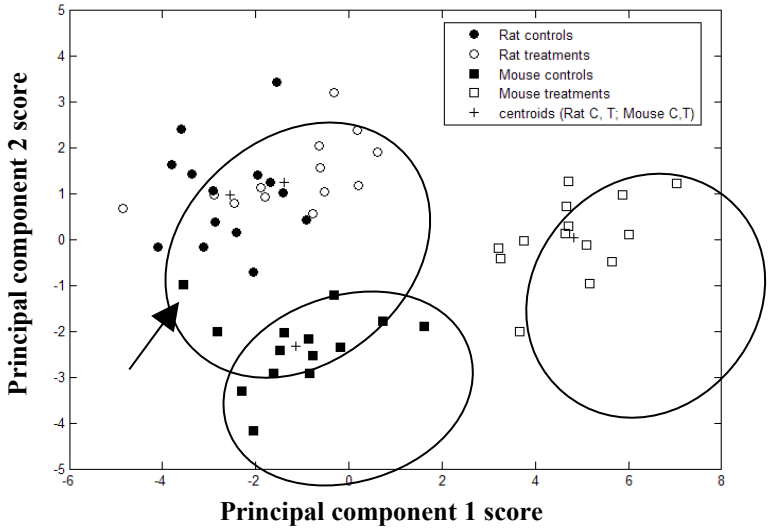

FIG. 2. PCA of combined rat and mouse datasets. The legend identifies symbols for rat and mouse controls and treated. The "+" symbols show location of centroid for controls and treatments.

3. Hepatic Lipids Analyzed by ^{13}C NMR Spectroscopy

Figure 3 shows a representative ^{13}C NMR spectrum of hepatic lipids indicating the regions of aliphatic, methyl, and olefinic carbons that come from fatty acids. The solvent signals from $CDCl_3$ and methanol are also identified. The $CDCl_3$ signal was used as a chemical shift reference and set to 77.79 ppm (relative to TSP at 0.0 ppm). This compound was also used for quantification purposes since its concentration in the sample is known.

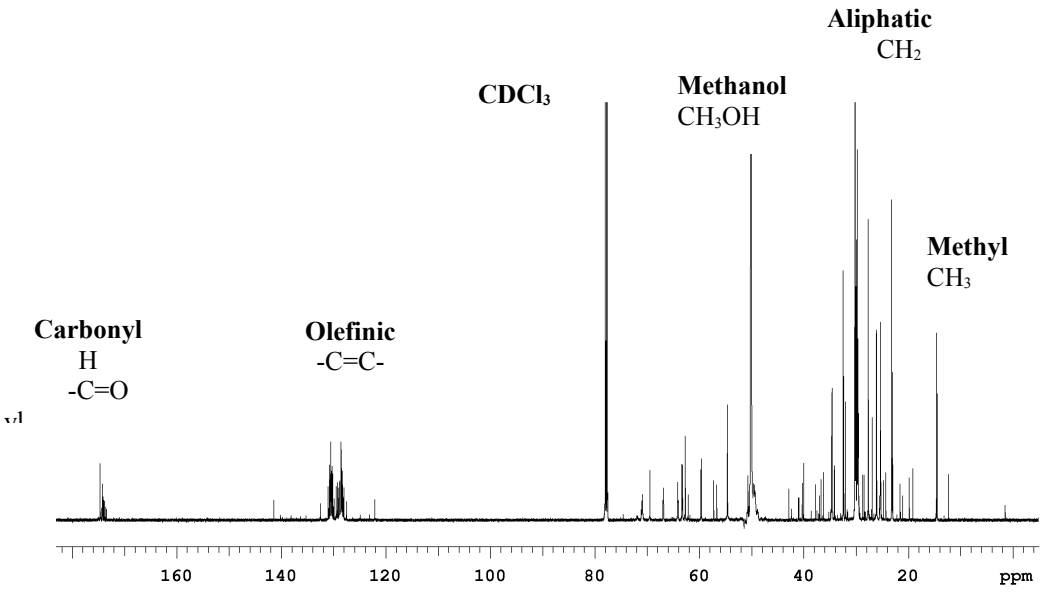

FIG. 3. Representative ^{13}C NMR spectrum of hepatic lipids showing the location of different carbons, for samples in a $CDCl_3$ solution.

TCDD induces changes in mean hepatic lipid metabolites. The peaks of interest in a ^{13}C NMR spectrum of lipid extracts include cholesterol, triacylglycerides (TAGs), and *n*3 and *n*6 fatty acids (FAs). An example of a ^{13}C NMR spectrum from a TCDD-treated mouse liver sample is shown in Figure 4. The main resonances in the ^{13}C NMR spectra of lipids were assigned according to the literature, and these are given in Table 3.

^{13}C NMR Spectrum of Hepatic Lipids

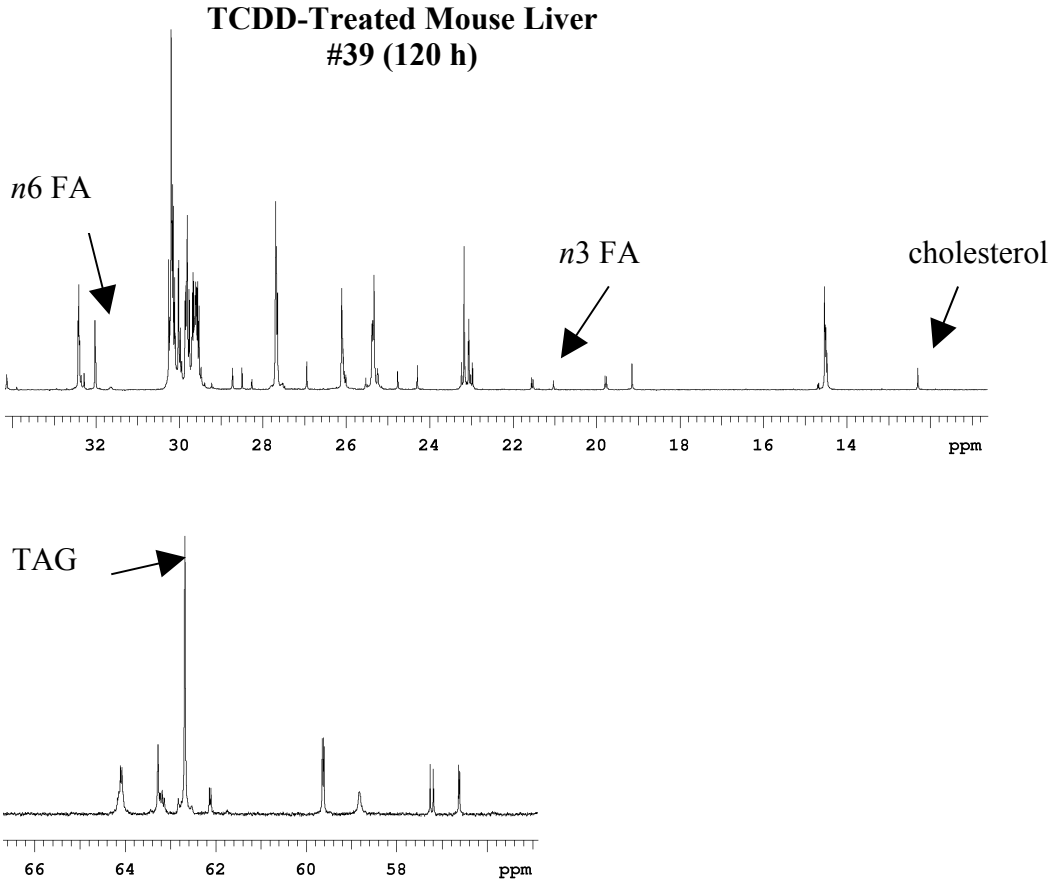

FIG. 4. An example of a ^{13}C NMR spectrum of lipids from a TCDD-treated mouse liver sample at 120 hours. Abbreviations: TAG, triacylglyceride; FA, fatty acid.

TABLE 3. Chemical shifts or ranges (on the ppm scale) of common carbon-functional groups observed in ^{13}C NMR spectra of mouse and rat liver lipid extracts, referenced to the center peak of $CDCl_3$ at 77.79 ppm. Bold denotes the location of the carbon in the chain represented by that peak or peak range.

Chemical shift (ppm)	Molecule	Assignment
32.0-32.3	*n*6 FA	C5 (C=C-**C**H_2-CH_2-CH_2-CH_2-CH_3)
21.0-21.3	*n*3 FA	C2 (-C=C-**C**H_2-CH_3)
12.5	Cholesterol	methyl group
62.6	TAG	1,3 **C** on glycerol backbone

Table 4 shows the saturation factors calculated when analyzing the ^{13}C NMR spectra of lipid extracts. NMR was run under fully relaxed (FR), and partially saturated (PS) conditions, and integrals for each metabolite of interest was obtained, to calculate the saturation factor for each metabolite.

TABLE 4. Saturation factors of specific lipid signals analyzed by ^{13}C NMR spectroscopy. All values were expressed as a ratio of integrated intensity relative to the $CDCl_3$ triplet. FR=fully relaxed data, PS=partially saturated data, SF=saturation factor=FR/PS.

	FR	PS	SF
***n*3**	0.192	2.96	0.0648
***n*6**	0.709	15.8	0.0450
TAG	0.821	29.5	0.0278
Cholesterol	0.0862	3.19	0.0271
PtdC from ^{13}C	0.678	29.2	0.0232

After identifying changes in metabolites from the spectra, and the metabolites using previous findings of ppm values from our lab as well as literature, the next step was to quantify these levels. Mean hepatic levels are depicted in graphic form.

a. Effects of TCDD on Mean Hepatic Triacylglycerides and Cholesterol

1.) Hepatic Triacylglycerides

Figure 5 shows how the mean levels of hepatic triacylglycerides (TAG) change over time, in vehicle control and TCDD-treated animals. The three-factor ANOVA shows that the data in the whole model is significant ($p<0.0001$). Species and treatment are significant, independent of time ($p<0.0001$). TAG levels in treated mice are two to three-folds higher than levels in controls. Differences in mean TAG levels in treated *vs*. control rats are not significant ($p=0.0937$).

There is a significant time effect ($p=0.0350$); levels increase from 72 to 168 hours. The one-factor ANOVA shows that this increase is in control rats ($p=0.0388$), and that neither group of mice change significantly across time. The three-factor ANOVA is more rigorous than the one-factor ANOVA, so these findings suggest that mean TAG levels are significantly higher in TCDD-treated mice than rats.

2.) Hepatic Cholesterol

According to the three-factor ANOVA, the data in the whole model for mean cholesterol levels shows significant changes ($p=0.0384$). The analysis indicates that

species and treatment groups show significant differences (p=0.0505), but not over time (p=0.1703). Significant changes in mean cholesterol levels occur in control and treated mice, but not rats (Figure 5). Mean cholesterol levels in TCDD-treated mice are 21-39% higher than levels in control mice at all times post-dose. The one-factor ANOVA shows that TCDD-treated mice have 39% higher mean levels of cholesterol compared to control mice at 72 hours (p=0.0132). Thus, TCDD induces an increase in cholesterol in mice but not rats.

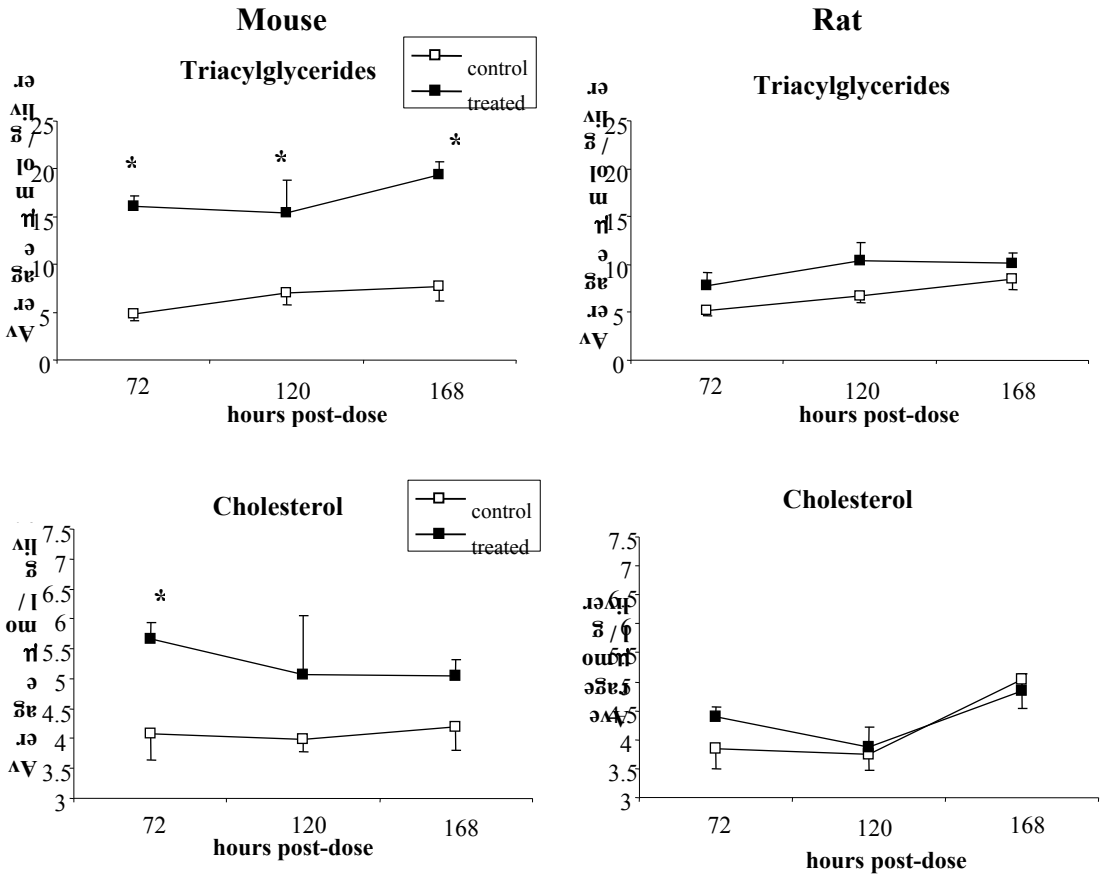

FIG. 5. Mean hepatic triacylglycerides and cholesterol levels (μmol/g liver; mean ± SE; *n*=4-5) measured by ^{13}C NMR spectroscopy in mice and rats as a function of time post-dose with TCDD. Empty boxes represent vehicle controls, and filled boxes treated animals. Bars represent ± standard error from the mean. The asterisk denotes a significant difference in treated *vs*. control at the specified time (p≤0.05). See Table 6 for statistical differences across time.

b. Effects of TCDD on Mean Hepatic *n*3 and *n*6 Fatty Acids

1.) Hepatic *n*3 Fatty Acids

The three-factor ANOVA shows that the data in the whole model of hepatic *n*3 fatty acids (FAs) is not significantly different (p=0.2665) (Figure 6). The one-factor ANOVA shows that levels of *n*3 FAs increase by 41% in mice at 72 hours (p=0.0127). There was no significant effect on hepatic *n*3 FAs in rats.

2.) Hepatic *n*6 FAs

The data in the whole model ANOVA of hepatic *n*6 FAs is significant, according to the three-factor ANOVA (p=0.0049). The only significant change in mean levels occurs between control and treated animals (p<0.0001) (Figure 6). This test does not indicate in which species or at what time post-dose. Mean levels of *n*6 FAs are significantly higher in treated animals relative to controls. The one-factor ANOVA shows that TCDD induces changes in mean levels of this metabolite in both rats and mice. Mean levels of *n*6 FAs in TCDD-treated mice relative to controls are 57% higher at 72 hours and 36% higher at 168 hours (p=0.0028). Rats at 120 hours have 41% higher mean levels compared to controls (p=0.0246). There is great variability in treated mice at 120 hours, which may explain why the time effect was not significant (p=0.1259). The three-factor ANOVA may show a significant species effect if the number of mice, or *n*, were increased. The analyses show that TCDD affects mean hepatic levels of this metabolite in both mice and rats.

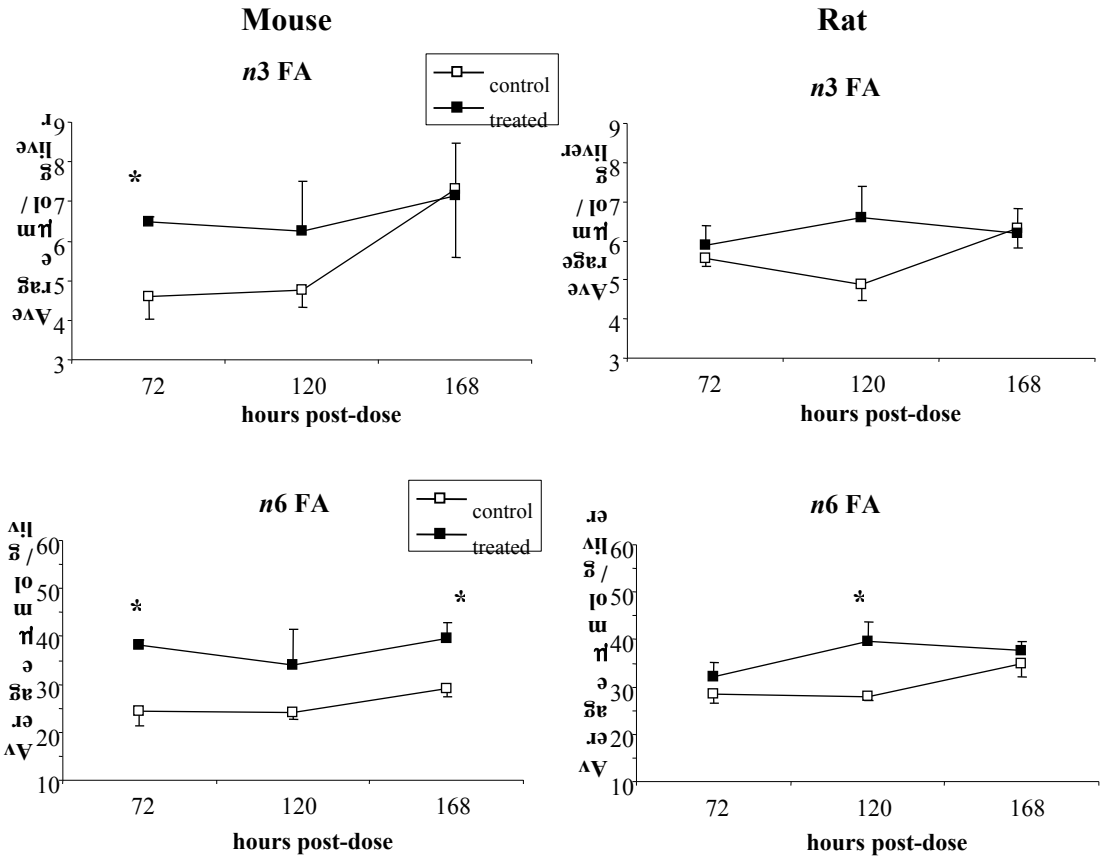

FIG. 6. Mean hepatic *n*3 and *n*6 fatty acids levels (μmol/g liver; mean ± SE; *n*=4-5) measured by ^{13}C NMR spectroscopy in mice and rats as a function of time post-dose with TCDD. Empty boxes represent vehicle controls, and filled boxes treated animals. Bars represent ± standard error from the mean. The asterisk denotes a significant difference in treated *vs*. control at the specified time ($p \leq 0.05$). See Table 6 for statistical differences across time.

Summary of Lipid Quantities Analyzed by ^{13}C NMR Spectroscopy

Table 5 summarizes the quantities of hepatic lipid metabolites analyzed by ^{13}C NMR spectroscopy. These quantities are mean levels, in μmol/g liver, obtained at each time post-dose and between treatment groups. Mean levels in treated and vehicle control rats and mice can be compared directly from this table. Table 6 shows the significant differences across time, in mean levels of these metabolites.

TABLE 5. Mean levels of hepatic lipid metabolites measured by ^{13}C NMR spectroscopy from TCDD-treated and vehicle control mice and rats at 72, 120, and 168 h post-dose (Mean ± SE; µmol/g liver; *n*=4-5 per group). The asterisk denotes significant differences ($p \leq 0.05$) between TCDD-treated and vehicle control animals at the specified time post-dose (one-factor ANOVA with post-hoc Tukey-Kramer Honestly Significant Difference). C=control, T=treated, h=hour.

Metabolite µmol/g liver	Mouse					
	72 h		120 h		168 h	
	C	T	C	T	C	T
TAG	4.87 ± 0.705	16.1 ± 1.01*	6.95 ± 1.15	15.4 ± 3.41*	7.75 ± 1.57	19.4 ± 1.35*
Cholesterol	4.07 ± 0.436	5.67 ± 0.259*	3.98 ± 0.211	5.07 ± 0.975	4.19 ± 0.385	5.05 ± 0.261
***n*3 FA**	4.60 ± 0.565	6.47 ± 0.155*	4.77 ± 0.457	6.25 ± 1.26	7.30 ± 1.71	7.14 ± 1.32
***n*6 FA**	24.3 ± 2.95	38.0 ± 1.36*	24.0 ± 1.41	34.1 ± 7.28	29.1 ± 1.58	39.7 ± 3.19*

Metabolite µmol/g liver	Rat					
	72 h		120 h		168 h	
	C	T	C	T	C	T
TAG	5.14 ± 0.465	7.79 ± 1.41	6.72 ± 0.710	10.4 ± 1.95	8.46 ± 1.10	10.1 ± 1.08
Cholesterol	3.84 ± 0.335	4.39 ± 0.168	3.74 ± 0.271	3.88 ± 0.346	5.03 ± 0.490	4.83 ± 0.308
***n*3 FA**	5.55 ± 0.215	5.88 ± 0.516	4.87 ± 0.399	6.60 ± 0.783	6.32 ± 0.508	6.19 ± 0.622
***n*6 FA**	28.6 ± 1.98	32.1 ± 2.91	28.0 ± 0.871	39.4 ± 4.34*	34.9 ± 2.91	37.5 ± 1.99

TABLE 6. Effect-derived differences in mean levels of specific hepatic lipids measured by ^{13}C NMR spectroscopy (μmol/g liver) for treatment, species, and time. Statistical significance was determined as in Table 2. *n*3 FAs did not show significant differences. M= mouse, R=rat, T=treated, C=control, h=hour post-dose, NS= no significant difference detected, NA=not appropriate. The p-values are not adjusted for multiple testing.

	Treatment (treated *vs.* control)			**Species (mouse *vs.* rat)**			**Time (72 h *vs.* 120 h *vs.*168 h)**		
	Main Effect (M + R)	**M**	**R**	**Main Effect (T + C)**	**T**	**C**	**Main Effect (M + R)**	**M**	**R**
TAG	NA	T > C 2-3-fold ($p<0.0001$)	NS	NA	M > R 1.5-2.1-fold ($p<0.0001$)	NS	72 h<168 h ($p=0.0350$)	NS	NS
Cholesterol	NA	T > C 21-39% ($p=0.0505$)	NS	NS	NS	NS	NS	NS	NS
***n*6 FA**	T > C ($p<0.0001$)	NS	NS	NS	NS	NS	NS	NS	NS

4. Hepatic Phospholipids Analyzed by ^{31}P NMR Spectroscopy

Analysis of ^{31}P NMR spectra provided changes in phospholipids such as sphingomyelin (SphM), cardiolipin, phosphatidylethanolamine (PtdE), and phosphatidylserine (PtdS).

^{31}P NMR Spectrum of Hepatic Phospholipids

An example of a ^{31}P NMR spectrum of lipids is shown in Figure 7, from a TCDD-treated mouse liver sample at 72 hours post-dose. The locations of phospholipids analyzed in this study are indicated. Each peak represents the phosphate group on the phospholipids. The main resonances in the ^{31}P NMR spectra of lipids were assigned according to the literature, and these are given in Table 7.

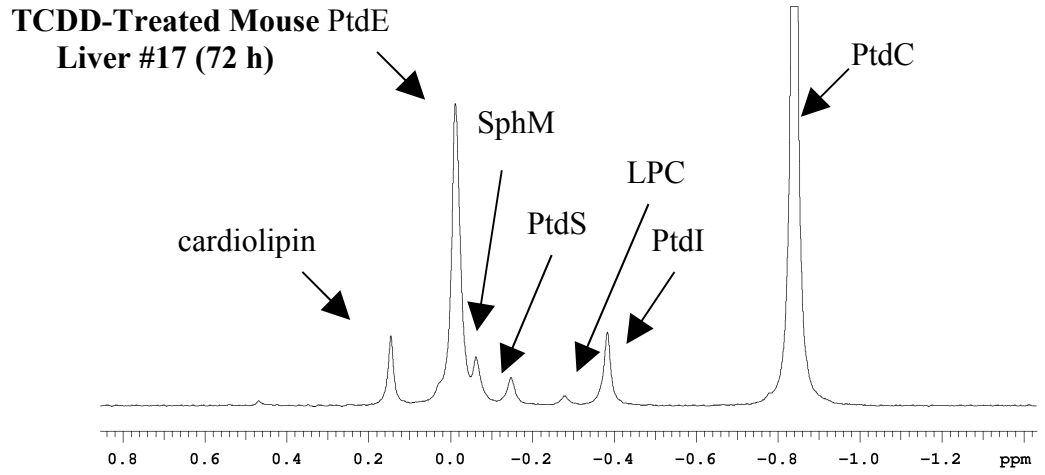

FIG. 7. Representative ^{31}P NMR spectrum of liver phospholipids in a TCDD-treated mouse liver sample #17, at 72 hours. Abbreviations: PtdE, phosphatidylethanolamine; SphM, sphingomyelin; PtdS, phosphatidylserine; LPC, lysophosphatidylcholine; PtdI, phosphatidylinositol; PtdC, phosphatidylcholine.

TABLE 7. Chemical shifts (on the ppm scale) of phosphates in phospholipids observed in mouse and rat liver lipid extracts in ^{31}P NMR spectra, referenced to PtdC at -0.84 ppm.

Chemical shift (ppm)	Molecule
0.18	Cardiolipin
0.0	PtdE
-0.08	SphM
-0.12	PtdS
-0.27	LPC
-0.38	PtdI
-0.84	PtdC

Table 8 shows the saturation factors calculated when analyzing the ^{13}P NMR spectra of lipid extracts.

TABLE 8. Saturation factors of specific lipid signals analyzed by ^{31}P NMR spectroscopy. All values were expressed as a ratio of integrated intensity relative to $CDCl_3$. FR=fully relaxed data, PS=partially saturated data, SF=saturation factor=FR/PS.

	FR	PS	SF
Cardiolipin			1
PtdS			1
PtdE			1
SphM			1

a. Effects of TCDD on Mean Hepatic Cardiolipin and Phosphatidylserine

1.) Hepatic Cardiolipin

The three-factor ANOVA shows that the data in the whole model of mean hepatic cardiolipin levels is significant (p=0.0269). Only vehicle control and TCDD-treated animals show significant changes in mean levels, independent of species or time (p=0.0004). Both treated animals have significantly lower, and similar, mean levels of cardiolipin compared to vehicle controls (Figure 8). The one-factor ANOVA shows that, at 168 hours, mean levels decrease by *ca*. 20% in both rats and mice (p=0.0113, 0.0320). The one-factor ANOVA reveals that mean levels do not change over time, in either mice or rats. Again, the great variability at 120 hours in treated mice may explain why no significant changes occurred over time (p=0.1968).

2.) Hepatic Phosphatidylserine

The data in the whole model of phosphatidylserine (PtdS) levels is significant (p=0.0040), using the three-factor ANOVA. Analysis of species, time, and treatment together show significant changes in mean PtdS levels (p=0.0522) (Figure 8). TCDD-treated rats have lower mean levels than control rats. The one-factor ANOVA across treatment shows that only rats exhibit significant changes; at 168 hours, mean PtdS levels are 43% lower in treated rats than in controls (p=0.0133). Also, control rats at 168 hours have significantly different mean levels from TCDD-treated rats at 72 and 120 hours; however, these are not different from treated rats at 168 hours. Mean hepatic levels in control rats at 168 hours and treated mice also differ significantly, but this comparison is irrelevant. Thus, only rats exhibit significantly lowered levels of mean PtdS levels with treatment at 168 hours post-dose. This metabolite was not present in the NMR spectra for every animal, so some groups had an *n*-value of only three.

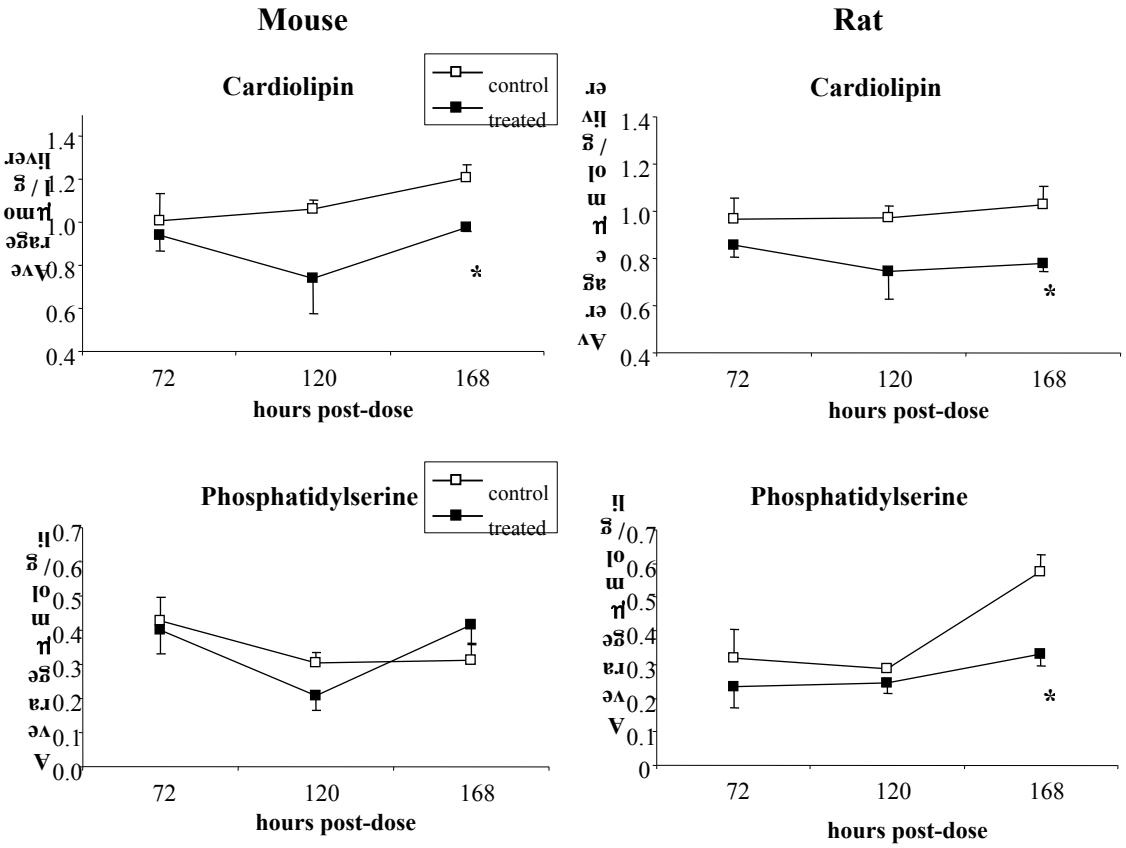

FIG. 8. Mean hepatic cardiolipin and phosphatidylserine levels (μmol/g liver; mean ±SE; *n*=3-5) measured by ^{31}P NMR spectroscopy in mice and rats as a function of time post-dose with TCDD. Empty boxes represent vehicle controls, and filled boxes treated animals. Bars represent ± standard error from the mean. The asterisk denotes a significant difference in treated *vs*. control at the specified time ($p \leq 0.05$). See Table 10 for statistical differences across time.

b. Effects of TCDD on Mean Hepatic Phosphatidylcholine and Phosphatidylethanolamine

1.) Hepatic Phosphatidylcholine

The three-factor ANOVA shows that the data in the whole model of hepatic phosphatidylcholine (PtdC) is not significant (p=0.2975) (Figure 9). The one-factor ANOVAs also show no significant differences in mean hepatic PtdC levels across treatment or time in either mice or rats. Thus, TCDD does not affect mean levels of PtdC in mice or rats.

2.) Hepatic Phosphatidylethanolamine

The data in the whole model of hepatic phosphatidylethanolamine (PtdE) is significant (p=0.0329). TCDD lowers mean PtdE levels to a greater extent in mice than in rats (p=0.0029) (Figure 9). However, this test does not indicate which treatment group exhibits this species effect. There is also a significant treatment effect (p=0.0097). Mean levels in TCDD-treated animals are lower than control levels, independent of species or time. TCDD-treated mice exhibit 27% lower mean levels of hepatic PtdE relative to controls only at 168 hours (p=0.0261).

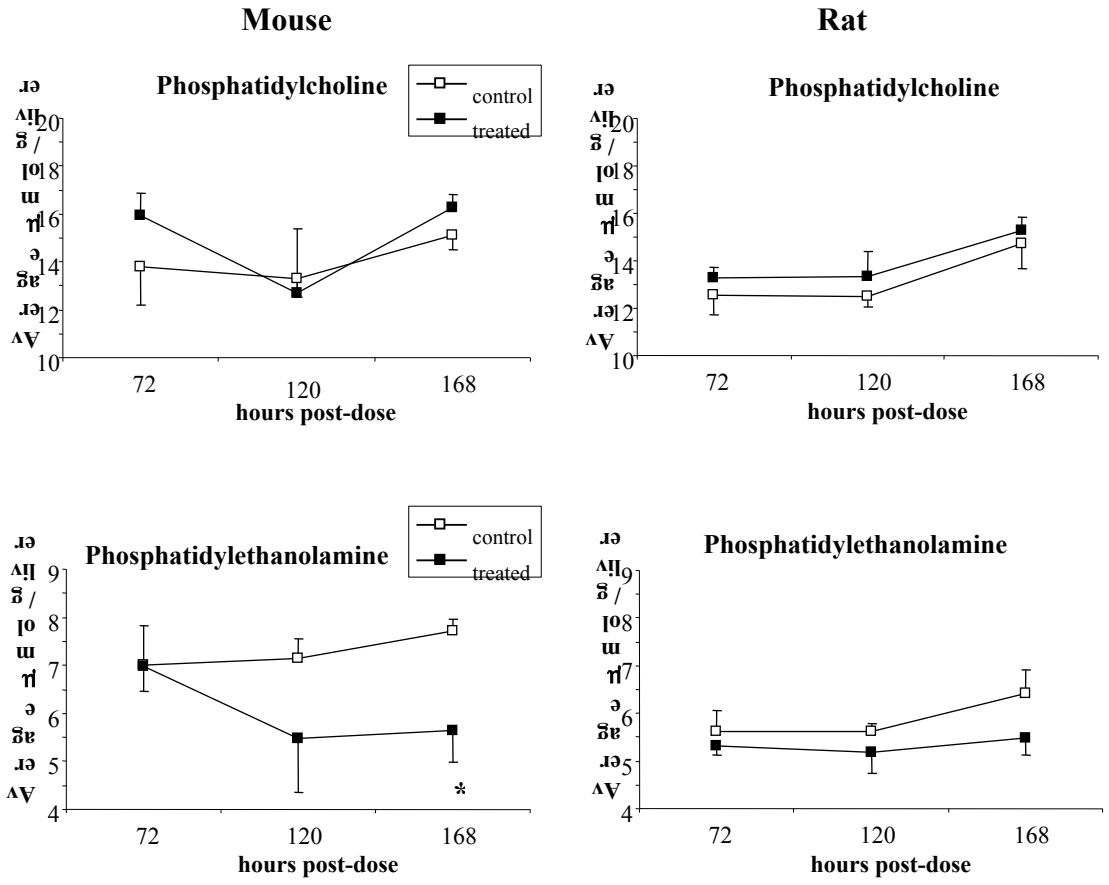

FIG. 9. Mean hepatic phosphatidylcholine and phosphatidylethanolamine levels (μmol/g liver; mean ± SE; *n*=4-5) measured by ^{31}P NMR spectroscopy in mice and rats as a function of time post-dose with TCDD. Empty boxes represent vehicle controls, and filled boxes treated animals. Bars represent ± standard error from the mean. The asterisk denotes a significant difference in treated *vs*. control at the specified time (p≤0.05). See Table 10 for statistical differences across time.

c. Effects of TCDD on the Mean Hepatic PtdC/PtdE Ratio

The PtdC/PtdE ratio was examined across time in both control and TCDD-treated species, and is illustrated in Figure 10. By the three-factor ANOVA, the data in the whole model is significant ($p<0.0001$). Significant differences occur with treatment and time ($p=0.0449$), and also with species ($p=0.0259$). The mean ratio in treated animals at 168 hours differs significantly from those at 72 and 120 hours. The mean ratio in treated animals at 168 hours is also different compared to that of controls at all times. However, this test does not indicate in which species these changes occur. The one-factor ANOVA shows that the ratio significantly increases in mice across treatment, by 17% at 72 ($p=0.0005$) and 23% at 120 hours ($p=0.0002$). There is great variability in the ratio in TCDD-treated mice at 168 hours. One animal had an almost two-fold higher ratio than the other animals in the same group (higher PtdC, lower PtdE), and this may explain this variability. Rats show significant changes in the ratio across treatment (12-22%) as well as across time ($p=0.0029$, 0.0007, 0.0023).

The species effect shows that the mean ratio is significantly greater in rats than mice. The one-factor ANOVA shows that the mean ratio in both control mice ($p=0.0027$) and treated rats ($p=0.0384$) significantly changes across time. Overall, TCDD causes an increase in the PtdC/PtdE ratio in both rats and mice, and it appears that the effect is of equal magnitude.

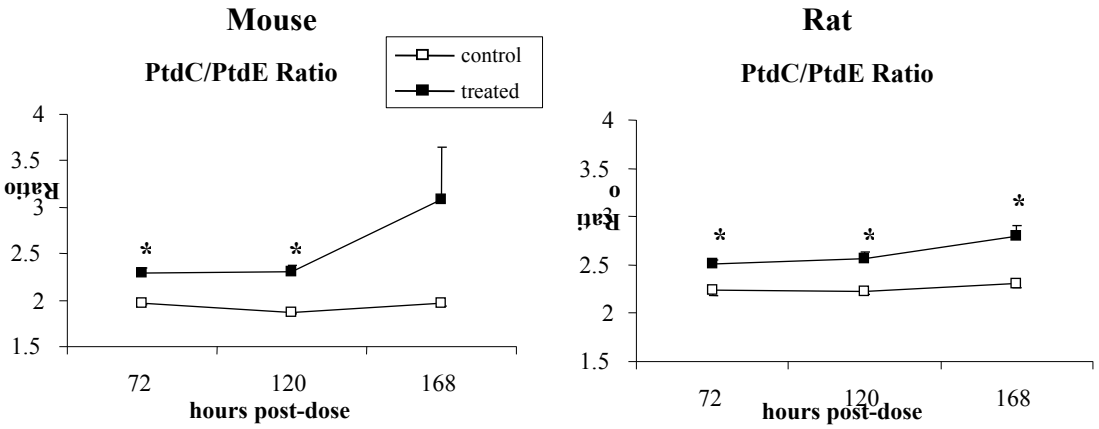

FIG. 10. TCDD-induced changes in the mean hepatic PtdC/PtdE ratio in mice and rats over time (mean ± SE; *n*=4-5). Empty boxes represent vehicle controls, and filled boxes treated animals. Bars represent ± standard error from the mean. The asterisk denotes a significant difference in treated *vs*. control at the specified time ($p \leq 0.05$). See Table 10 for statistical differences across time.

d. Effects of TCDD on the Mean Hepatic PtdS/PtdE Ratio

The PtdS/PtdE ratio was analyzed only in rats, and the one-factor ANOVA shows treatment and time effects. In treated rats at 168 hours, the ratio decreases by 36% relative to control rats ($p=0.0234$) (Figure 11). Control rats show a significant time effect ($p=0.0125$). As noted earlier, PtdS was not visible in the NMR spectra of each animal, and some groups only had three animals (*n*-value) for analysis.

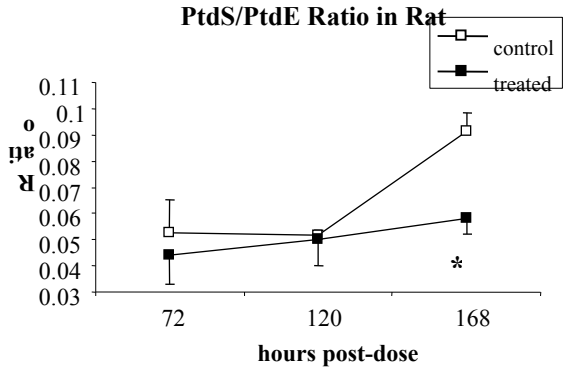

FIG. 11. TCDD-induced changes in the mean hepatic PtdS/PtdE ratio in rats over time (mean ± SE; *n*=3-5). Empty boxes represent vehicle controls, and filled boxes treated animals. Bars represent ± standard error from the mean. The asterisk denotes a significant difference in treated *vs*. control at the specified time ($p \leq 0.05$). See Table 10 for statistical differences across time.

e. Effects of TCDD on Mean Hepatic Sphingomyelin

The data in the whole model of hepatic sphingomyelin (SphM) levels is significant (p=0.0008), using the three-factor ANOVA. Species and treatment are significant (p=0.0041). Control and treated rats have different mean SphM levels, independent of time (Figure 12). Mean SphM levels in treated rats are 30-38% lower relative to control rats at all times. The one-factor ANOVA of treatment effects shows that TCDD-treated rats at 72 and 168 hours exhibit 30 and 38% lower mean levels of SphM relative to control rats, respectively. Mice do not show significant treatment effects.

The three-factor ANOVA shows a significant time effect (p=0.0031), at 72 and 120 hours, as well as at 120 and 168 hours. The one-factor ANOVA shows that mean levels in treated mice and control and treated rats significantly change across time. Mean SphM levels in treated mice decrease from 72 to 120 hours (p=0.0415), control rats increase from 120 to 168 hours (p=0.0288), and treated rats increase from 72 to 168 and 120 to 168 hours (p=0.0377).

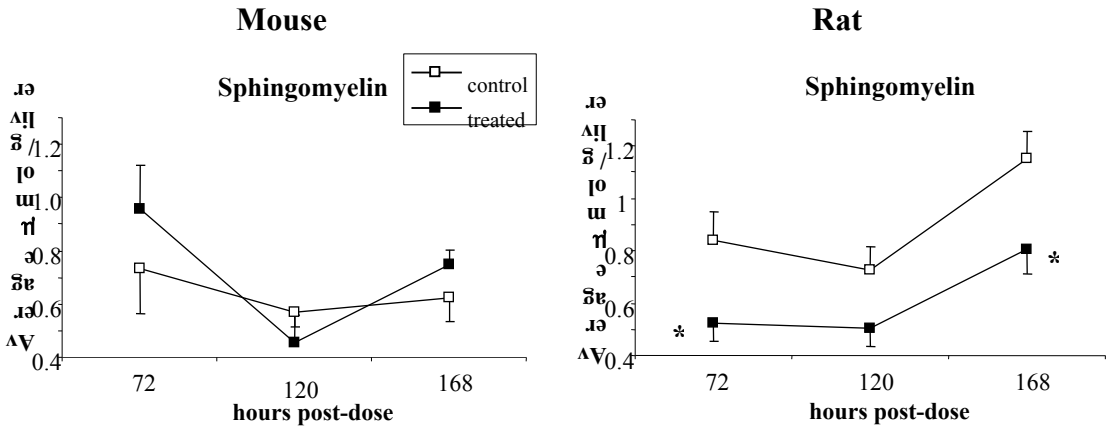

FIG. 12. Mean hepatic sphingomyelin levels (μmol/g liver; mean ± SE; *n*=4-5) measured by ^{31}P NMR spectroscopy in mice and rats as a function of time post-dose with TCDD. Empty boxes represent vehicle controls, and filled boxes treated animals. Bars represent ± standard error from

the mean. The asterisk denotes a significant difference in treated *vs*. control at the specified time ($p \leq 0.05$). See Table 10 for statistical differences across time.

Summary of Phospholipid Quantities Analyzed by ^{31}P NMR Spectroscopy

Table 9 summarizes the quantities of lipid metabolites analyzed by ^{31}P NMR spectroscopy. These quantities are mean levels of specific phospholipids, in μmol/g liver, obtained at each time post-dose and between treatment groups. Table 10 shows the significant differences across time, in mean levels of these metabolites.

TABLE 9. Mean levels of hepatic lipid metabolites measured by ^{31}P NMR spectroscopy from TCDD-treated and vehicle control mice and rats at 72, 120, and 168 h post-dose (Mean ± SE; µmol/g liver; *n*=4-5 per group). Also shown is the PtdC/PtdE ratio for mice and rats. The asterisk denotes significant differences ($p \leq 0.05$) between TCDD-treated and vehicle control animals at the specified time post-dose (one-factor ANOVA with post-hoc Tukey-Kramer Honestly Significant Difference). C=control, T=treated, h=hour.

Metabolite µmol/g liver	Mouse					
	72 h		120 h		168 h	
	C	T	C	T	C	T
Cardiolipin	1.01 ± 0.127	0.942 ± 0.0768	1.06 ± 0.0463	0.742 ± 0.163	1.21 ± 0.0605	0.980 ± 0.0182*
PtdS	0.429 ± 0.0674	0.401 ± 0.0706	0.303 ± 0.0328	0.206 ± 0.0396	0.311 ± 0.0474	0.415 ± 0.0540
PtdC	13.8 ± 1.59	15.9 ± 0.970	13.3 ± 0.780	12.7 ± 2.67	15.1 ± 0.598	16.3 ± 0.559
PtdE	7.01 ± 0.816	6.98 ± 0.527	7.13 ± 0.432	5.49 ± 1.13	7.70 ± 0.255	5.64 ± 0.654*
PtdC/PtdE	1.96 ± 0.0184	2.29 ± 0.0557*	1.87 ± 0.0133	2.31 ± 0.0681*	1.96 ± 0.0189	3.08 ± 0.566
SphM	0.731 ± 0.167	0.956 ± 0.166	0.569 ± 0.0522	0.456 ± 0.104	0.623 ± 0.0873	0.750 ± 0.0532

Metabolite µmol/g liver	Rat					
	72 h		120 h		168 h	
	C	T	C	T	C	T
Cardiolipin	0.967 ± 0.0874	0.855 ± 0.0474	0.971 ± 0.0532	0.746 ± 0.120	1.03 ± 0.0792	0.778 ± 0.0305*
PtdS	0.319 ± 0.0858	0.235 ± 0.0631	0.289 ± 0.00530	0.246 ± 0.0321	0.577 ± 0.0479	0.330 ± 0.0329*
PtdC	12.5 ± 0.833	13.3 ± 0.438	12.5 ± 0.474	13.3 ± 1.09	14.7 ± 1.03	15.3 ± 0.563
PtdE	5.62 ± 0.424	5.31 ± 0.196	5.62 ± 0.178	5.19 ± 0.450	6.42 ± 0.494	5.48 ± 0.346
PtdC/PtdE	2.24 ± 0.0478	2.51 ± 0.0420*	2.23 ± 0.0283	2.57 ± 0.0580*	2.30 ± 0.0376	2.80 ± 0.112*
PtdS/PtdE	0.0528 ± 0.0125	0.0443 ± 0.0115	0.0514 ± 0.00241	0.0500 ± 0.00979	0.0914 ± 0.00705	0.0583 ± 0.00604*
SphM	0.840 ± 0.108	0.522 ± 0.0696*	0.728 ± 0.0863	0.502 ± 0.0679	1.15 ± 0.104	0.807 ± 0.0941*

TABLE 10. Effect-derived differences in mean levels of specific hepatic phospholipids measured by ^{31}P NMR spectroscopy (μmol/g liver) for treatment, species, and time. Also shown are differences in the PtdC/PtdE ratio. Statistical significance was determined as in Table 2. PtdC and PtdI did not show significant differences. PtdS showed significant, but seemingly irrelevant differences, between control rat at 168 h *vs.* treated rat at 72 h, treated rat at 120 h, and treated mouse at 120 h. SphM also showed significant differences between treatment, time, and species. At 72 h, SphM levels differed between control mouse and rat, treated mouse and rat, and control and treated mouse. Also, treated mouse at 72 h were different from 120 and 168 h. Treated mouse and rats differed at 168 h. M= mouse, R=rat, T=treated, C=control, h=hour post-dose, NS= no significant difference detected, NA=not appropriate. The p-values are not adjusted for multiple testing.

	Treatment (treated *vs.* control)			**Species (mouse *vs.* rat)**			**Time (72 h *vs.* 120 h *vs.* 168 h)**		
	Main Effect (M + R)	**M**	**R**	**Main Effect (T + C)**	**T**	**C**	**Main Effect (M + R)**	**M**	**R**
Cardiolipin	T < C (p=0.0004)	NS	NS	NS	NS	NS	NS	NS	NS
PtdE	T < C (p=0.0097)	NS	NS	M > R (p=0.0029)	NS	NS	NS	NS	NS
PtdC/PtdE	NS	NS	NS	M < R (p=0.0259)	NS	NS	NS	NS	NS
SphM	NA	NS	T < C 30-38% (p=0.0041)	NA	NS	M > R 15-85% (p=0.0041)	NA	72 h>120 h (p=0.017)	120 h<168 h (p=0.017)

B. AQUEOUS EXTRACTS

TCDD also induces changes in hepatic aqueous metabolites. The metabolite profiles in aqueous samples were analyzed by ^{1}H and ^{31}P NMR spectroscopy. ^{31}P NMR spectra of aqueous extracts yielded amounts of glucose-6-phosphate (G6P), glycerophosphocholine (GPC), glycerophosphoethanolamine (GPE), phosphocholine (Pcho), phosphoethanolamine (Peth), and glycerol-3-phosphate (G3P).

1. Effects of TCDD on Mean Total Hepatic Aqueous Extracts

Figure 13 shows how the content of dried extract from the aqueous phase of the liver extract (mg aqueous/g liver) changes in vehicle control and TCDD-treated animals at each time post-dose. However, most of the weight is likely salts. The data in the whole model is significant when using the three-factor ANOVA ($p=0.0011$) (Figure 13). Species, time, and treatment together are significant ($p=0.0182$). At 72 hours, control mice have 59% higher mean aqueous content than control rats. Control mice at this time have great variability, due to one mouse liver sample (control #12) having unusually higher mean aqueous content than the rest in the same group.

When conducting the one-factor ANOVA across treatment, with this control mouse liver sample #12 included, the treatment effect is not significant ($p=0.0965$). However, when this sample is omitted, mice show significant changes in mean content between control and treatment at 72 ($p=0.0182$) and 120 hours ($p=0.0178$), and rats at 168 hours ($p=0.0367$). Also, the one-factor ANOVA shows that mean aqueous content in treated mice ($p=0.0394$) and control rats ($p=0.0054$) significantly changes over time. Control mouse liver sample #12 (72 hours post-dose) was removed from the statistical analyses when examining significant changes in metabolites from the aqueous extracts.

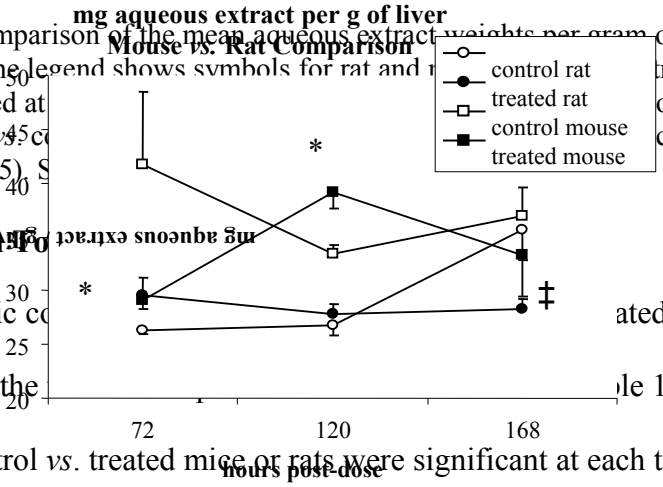

FIG. 13. Species comparison of the mean aqueous extract weights per gram of liver as a function of time post-dose. The legend shows symbols for rat and m treatment groups. Effects were examined at otes a significant difference in treated *vs*. c control rats, at the specified time ($p \leq 0.05$). S

Summary of Mean Fo

Mean hepatic co ated animals (mice and rats) at each of the le 11. The table also shows whether control *vs*. treated mice or rats were significant at each time post-dose.

TABLE 11. Mean hepatic content of aqueous extract in TCDD-treated and vehicle control mice and rats at 72, 120, and 168 h post-dose (Mean ± SE; mg aqueous content/g liver; *n*=3-5 per group). The asterisk denotes significant differences ($p \leq 0.05$) between TCDD-treated and vehicle control animals at the specified time post-dose (one-factor ANOVA with post-hoc Tukey-Kramer Honestly Significant Difference). C=control, T=treated, h=hour, aq=aqueous).

	Mouse					
	72 h		**120 h**		**168 h**	
	C	**T**	**C**	**T**	**C**	**T**
Aqueous Content (mg aq/g liver)	35.2±2.09	29.1±0.751*	33.4±0.858	39.1±1.51*	36.9±2.72	33.3±3.89

	Rat					
	72 h		**120 h**		**168 h**	
	C	**T**	**C**	**T**	**C**	**T**
Aqueous Content (mg aq/g liver)	26.3±0.335	29.6±1.63	26.8±0.947	27.8±1.01	35.6±2.78	28.3±0.946*

2. Hepatic Metabolites Analyzed by ^{31}P NMR Spectroscopy of Aqueous Extracts

There was one mouse liver sample (control mouse #32), at the 168-hour time-point that needed to be removed from the ^{31}P NMR spectroscopy analysis of aqueous extracts. Several peaks were broadened, and it is believed to be due to paramagnetic cations remaining in the sample not completely removed by the chelex. Unfortunately, this lowered the *n*-value for control mice at the 168-hour post-dose to three.

^{31}P NMR Spectrum of Hepatic Aqueous Metabolites

An example of a ^{31}P NMR spectrum of aqueous metabolites from a treated mouse liver is shown in Figure 14. Table 12 shows the chemical shifts of metabolites identified in the ^{31}P NMR spectra of aqueous extracts. All ^{31}P NMR spectra were referenced to GPC at 3.082 ppm. Metabolites were identified using ppm values obtained from the literature.

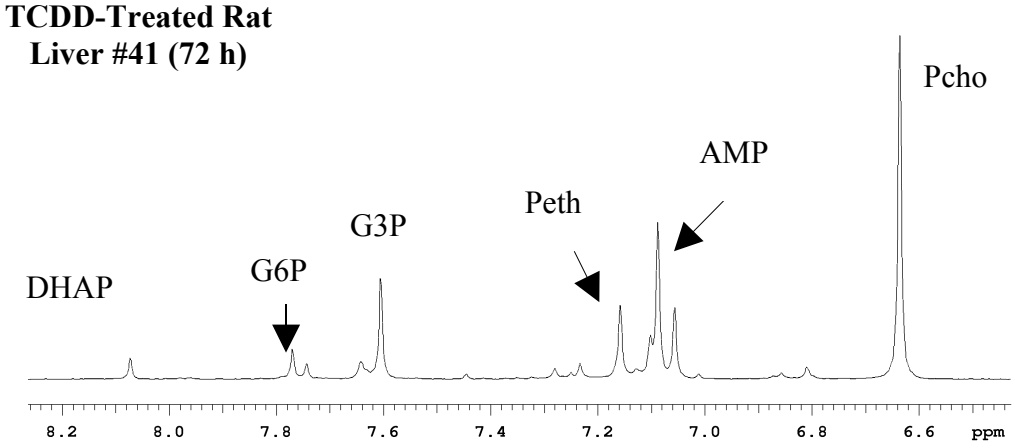

FIG. 14. ^{31}P NMR spectrum of aqueous metabolites in a TCDD-treated rat liver sample at 72 hours. Abbreviations: DHAP, dihydroxyacetone phosphate; G6P, glucose-6-phosphate; G3P, glycerol-3-phosphate; Peth, phosphoethanolamine; Pcho, phosphoethanolamine.

TABLE 12. Chemical shifts (on the ppm scale) of phosphates observed in mouse and rat in ^{31}P NMR spectra of aqueous liver extracts, referenced to GPC at 3.082 ppm.

Chemical shift (ppm)	Molecule
3.082	GPC
3.44	GPE
5.17	Pi
6.67	Pcho
7.1	AMP
7.07	Peth
7.62	G3P
7.79	G6P
8.05	DHAP

Table 13 shows the saturation factors calculated when analyzing the ^{13}P NMR spectra of aqueous extracts.

TABLE 13. Saturation factors of specific aqueous metabolite signals analyzed by ^{31}P NMR spectroscopy. All values were expressed as a ratio of integrated intensity relative to MDPA for ^{31}P NMR spectroscopy. FR=fully relaxed data, PS=partially saturated data, SF=saturation factor=FR/PS.

^{31}P metabolite	FR	PS	SF
DHAP	2.05	1.34	1.53
G6P	5.14	4.86	1.06
G3P	19.4	16.5	1.18
Pcho	30.1	25.1	1.20
Peth	4.98	4.25	1.17
GPC	2.60	2.73	0.954
GPE	4.12	4.18	0.986

a. Effects of TCDD on Mean Hepatic DHAP and Glycerol-3-Phosphate

1.) Hepatic DHAP

When using the three-factor ANOVA to examine whether significant changes occur in mean levels of hepatic DHAP, the data in the whole model is not significant ($p=0.2912$) (Figure 15). However, the one-factor ANOVA shows that mean DHAP levels in TCDD-treated mice are 49% lower than in control mice at 168 hours ($p=0.0469$). No significant changes occur across time in either species.

2.) Hepatic Glycerol-3-Phosphate

The data in the whole model for glycerol-3-phosphate (G3P) is significant, according to the three-factor ANOVA ($p=0.0024$). There is a significant species and time

effect (p=0.0095), but differences between treatment are not significant (p=0.4919) (Figure 15). In mice, levels of G3P significantly decrease from 120 to 168 hours. Mean hepatic G3P levels in mice at 120 hours also differ from rats at each time post-dose, but this is irrelevant. The one-factor ANOVA shows no significant changes in either species across treatment. However, there is a significant time effect in treated mice (p=0.0177).

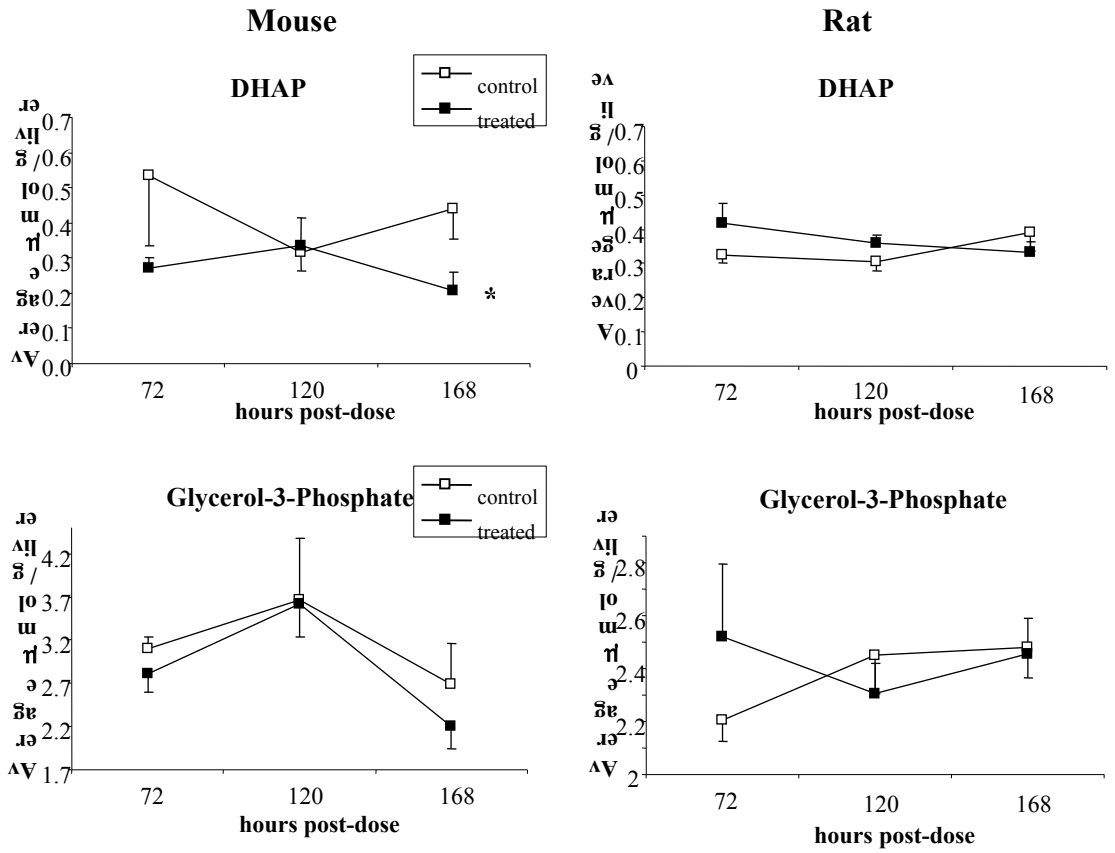

FIG. 15. Mean hepatic DHAP and glycerol-3-phosphate levels (µmol/g liver; mean ± SE; *n*=3-5) measured by ^{31}P NMR spectroscopy in mice and rats as a function of time post-dose with TCDD. Empty boxes represent vehicle controls, and filled boxes treated animals. Bars represent ± standard error from the mean. The asterisk denotes a significant difference in treated *vs*. control at the specified time (p≤0.05). See Table 15 for statistical differences across time.

b. Effects of TCDD on the Mean Hepatic G3P/DHAP Ratio

Figure 16 shows how the mean G3P/DHAP ratio varies across time in each species. The reduced/oxidized form of the ratio provides information about the cytosolic redox potential. The three-factor ANOVA indicates that the data in the whole model is

significant (p=0.0038). There is only a significant species effect (p=0.0005); mice appear to have higher mean ratios than rats. This species effect is independent of treatment or time. The one-factor ANOVAs across treatment or time prove not significant.

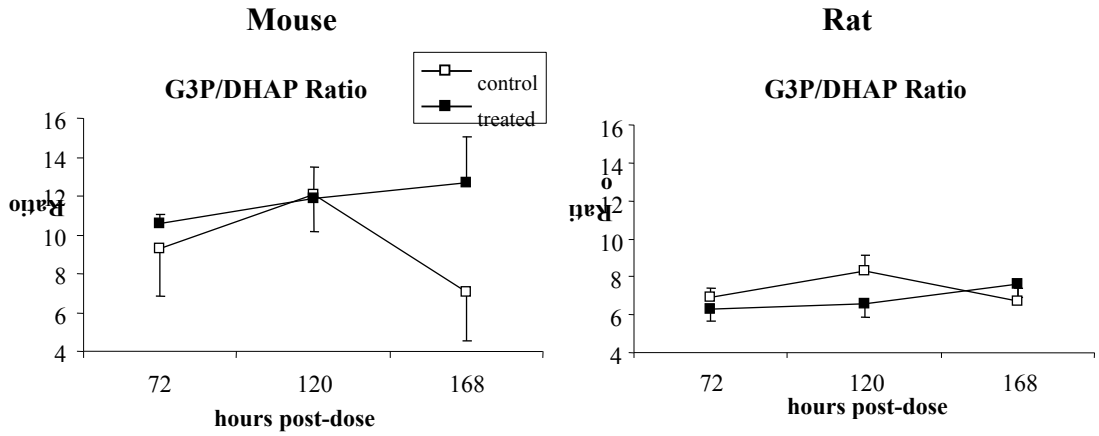

FIG. 16. TCDD-induced changes in the G3P/DHAP ratio measured by ^{31}P NMR spectroscopy in mice and rats as a function of time post-dose with TCDD (mean ± SE; *n*=3-5). Empty boxes represent vehicle controls, and filled boxes treated animals. Bars represent ± standard error from the mean. The asterisk denotes a significant difference in treated *vs*. control at the specified time ($p \leq 0.05$). See Table 15 for statistical differences across time.

c. Effects of TCDD on Mean Hepatic Glucose-6-Phosphate

The data in the whole model for hepatic glucose-6-phosphate (G6P) levels shows significant TCDD-induced effects (p=0.0112). There is a significant treatment effect, mean levels of G6P falling after administration of TCDD (p=0.0066) (Figure 17). There is also a significant species effect (p=0.0019). According to the one-factor ANOVA, at 120 hours, mean G6P levels in treated rats are 29% lower than mean levels in control rats (p=0.0321). Control and treated mice are not significantly different, perhaps due to control mice showing greater variability at 120 hours. The analysis also shows that mean G6P levels in treated mice differ significantly across time (p=0.0595).

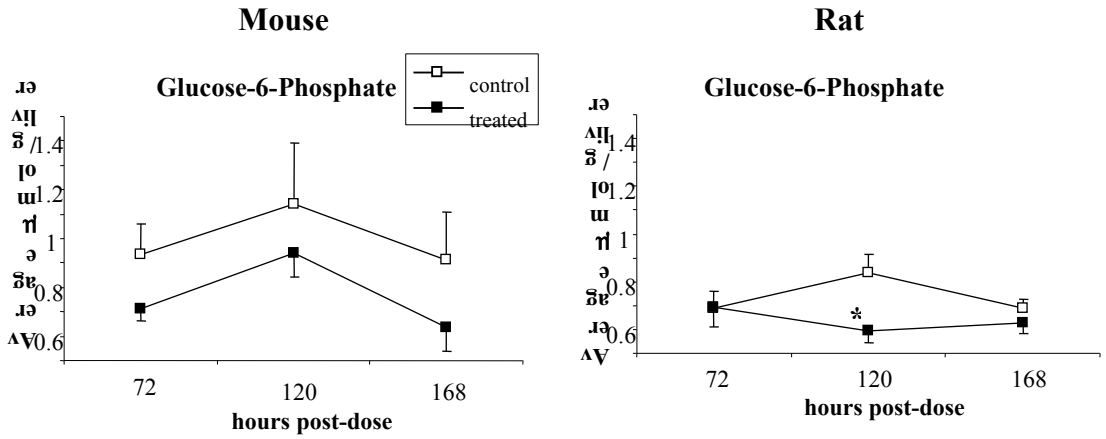

FIG. 17. Mean hepatic glucose-6-phosphate levels (μmol/g liver; mean ± SE; *n*=3-5) measured by ^{31}P NMR spectroscopy in mice and rats as a function of time post-dose. Empty boxes represent vehicle controls, and filled boxes treated animals. Bars represent **±** standard error from the mean. The asterisk denotes a significant difference in treated *vs*. control at the specified time ($p \leq 0.05$). See Table 15 for statistical differences across time.

d. Effects of TCDD on Mean Hepatic Phosphocholine and Phosphoethanolamine

1.) Hepatic Phosphocholine

The three-factor ANOVA shows the data in the whole model for hepatic phosphocholine (Pcho) ($p<0.0001$). There is a significant species and treatment effect, independent of time ($p<0.0001$). Figure 18 clearly shows that the mean Pcho levels are different between control and treated rats. Mean Pcho levels are 2.6-3.2-folds higher in TCDD-treated rats than those in control rats, at all times post-dose. The one-factor ANOVA shows that in rats, mean Pcho levels are significantly different between control and treated groups at all times ($p=0.0052$, <0.0001, <0.0001). This treatment effect is not observed in mice.

These findings indicate that TCDD greatly induces mean Pcho levels in rats and not mice. The three-factor ANOVA shows no significant time effects ($p=0.9690$), however, the one-factor analysis shows that mean Pcho levels in treated mice differ significantly across time ($p=0.0205$).

2.) Hepatic Phosphoethanolamine

The data in the whole model of hepatic phosphoethanolamine (Peth) shows significant differences (p=0.0229). Significant changes occur with species, time, and treatment together (p=0.0118), but the Tukey test failed to specify which factor (Figure 18). The Tukey test may show significant effects if the *n*-value is increased.

The one-factor ANOVA shows that mean Peth levels significantly change between control and treated rats at 120 hours (p=0.0229). Levels in treated rats are 20% lower than levels in control rats. Only TCDD-treated mice change over time (p=0.0042).

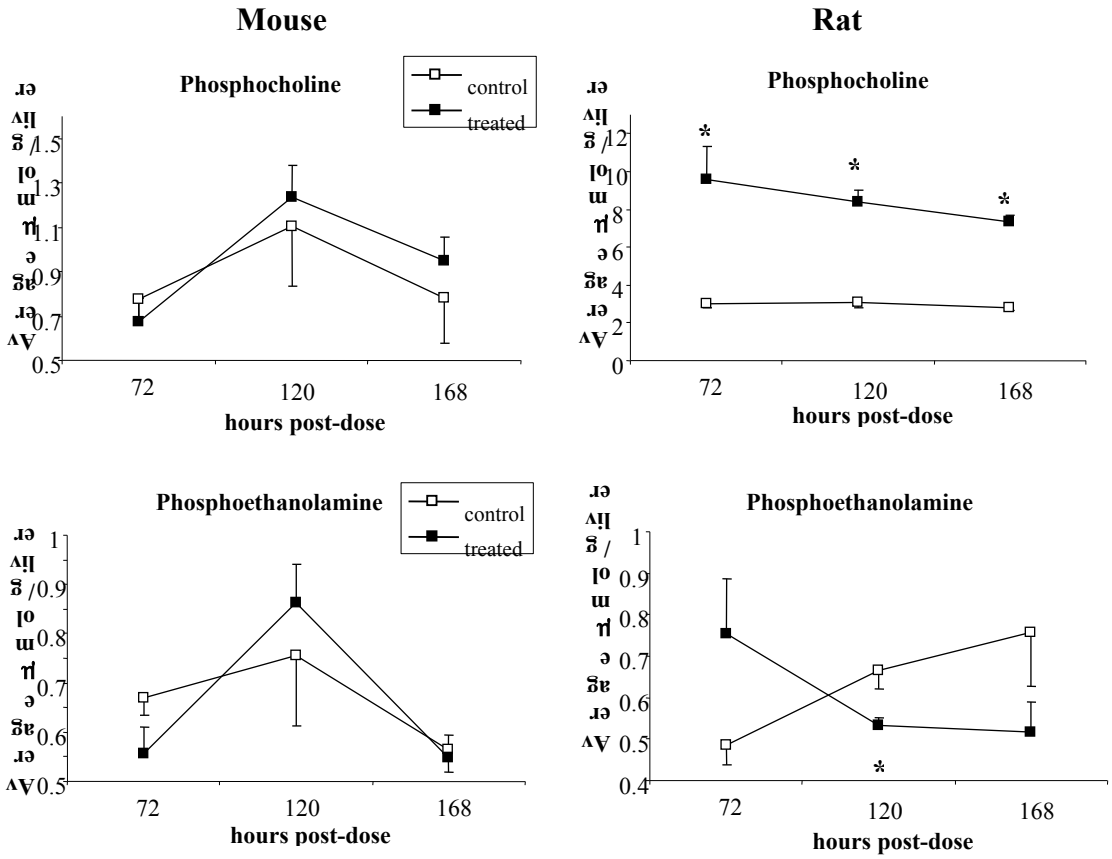

FIG. 18. Mean hepatic phosphocholine and phosphoethanolamine levels (μmol/g liver; mean ± SE; *n*=3-5) measured by ^{31}P NMR spectroscopy in mice and rats as a function of time post-dose. Empty boxes represent vehicle controls, and filled boxes treated animals. Bars represent ± standard error from the mean. The asterisk denotes a significant difference in treated *vs*. control at the specified time (p≤0.05). See Table 15 for statistical differences across time.

e. Effects of TCDD on Mean Hepatic Glycerophosphocholine and Glycerophosphoethanolamine

1.) Hepatic Glycerophosphocholine

The three-factor analysis of mean glycerophosphocholine (GPC) levels shows that the data in the whole model is significant ($p=0.0020$). Significant changes occur with treatment and species ($p=0.0465$), but these comparisons are irrelevant (control rats *vs*. control mice, and treated rats *vs*. control mice) (Figure 19). There is no significant time effect ($p=0.1315$).

The one-factor ANOVA shows that only at the 168-hour time post-dose, GPC levels in treated mice are significantly lower (26%) than those in control mice ($p=0.0334$). Time effects are not significant in either species.

2.) Hepatic Glycerophosphoethanolamine

Analysis of mean glycerophosphoethanolamine (GPE) levels using the three-factor ANOVA shows that the data in the whole model is significant ($p<0.0001$). There is only a significant species effect, independent of treatment or time (Figure 19). Mean levels of this metabolite are greater in rats than in mice ($p<0.0001$).

The one-factor ANOVA shows that mean GPE levels do not change significantly across treatment in either species, and that treated mice show a significant effect across time ($p=0.0072$).

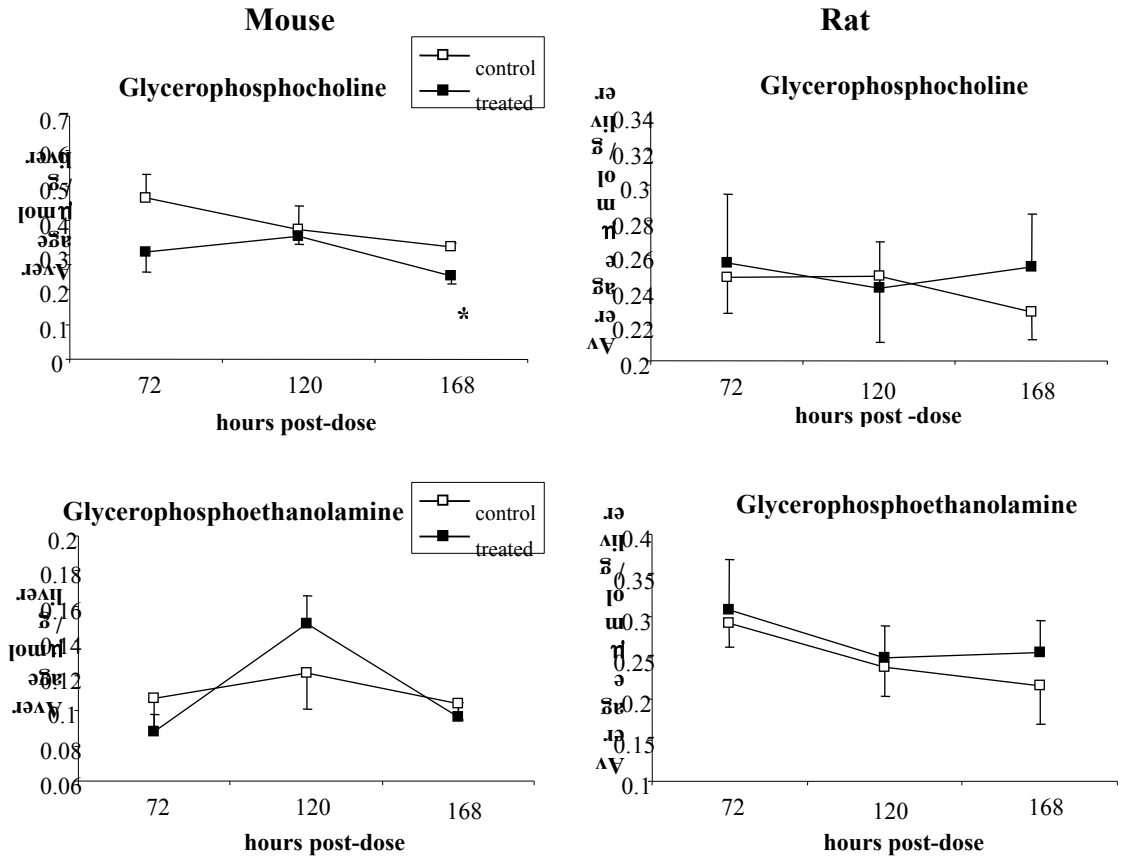

FIG. 19. Mean hepatic glycerophosphocholine and glycerophosphoethanolamine levels (μmol/g liver; mean ± SE; *n*=3-5) measured by ^{31}P NMR spectroscopy in mice and rats as a function of time post-dose. Empty boxes represent vehicle controls, and filled boxes treated animals. Bars represent ± standard error from the mean. The asterisk denotes a significant difference in treated *vs*. control at the specified time ($p \leq 0.05$). See Table 15 for statistical differences across time.

Summary of Metabolite Quantities Analyzed by ^{31}P NMR Spectroscopy of Aqueous Extracts

Table 14 summarizes the mean quantities of metabolites analyzed by ^{31}P NMR spectroscopy of hepatic aqueous extracts, in μmol/g liver. This is to facilitate species comparison. Table 15 shows the significant differences across time.

TABLE 14. Mean levels of hepatic metabolites measured by ^{31}P NMR spectroscopy of aqueous extracts from TCDD-treated and vehicle control mice and rats at 72, 120, and 168 hours post-dose (Mean ± SE; µmol/g liver; *n*=3-5 per group). Also shown is the G3P/DHAP ratio for mice and rats. The asterisk denotes significant differences ($p \leq 0.05$) between TCDD-treated and vehicle control animals at the specified time post-dose (one-factor ANOVA with post-hoc Tukey-Kramer Honestly Significant Difference). C=control, T=treated, h=hour.

Metabolite µmol/g liver	Mouse					
	72 h		120 h		168 h	
	C	T	C	T	C	T
DHAP	0.536±0.202	0.271±0.0288	0.316±0.0505	0.337±0.0762	0.439±0.0849	0.208±0.0517*
G3P	3.09±0.143	2.81±0.221	3.66±0.720	3.62±0.382	2.69±0.476	2.20±0.258
G3P/DHAP	9.28±2.44	10.6±0.497	12.1±1.91	11.9±1.62	7.04±2.48	12.6±2.40
G6P	0.937±0.123	0.711±0.0495	1.14±0.250	0.940±0.0971	0.914±0.194	0.636±0.0952
Pcho	0.778±0.0789	0.676±0.103	1.10±0.266	1.24±0.141	0.778±0.202	0.946±0.111
Peth	0.669±0.0340	0.558±0.0538	0.755± 0.143	0.864±0.0767	0.565±0.0458	0.549±0.0451
GPC	0.464±0.0689	0.307±0.0543	0.371±0.0719	0.354±0.0217	0.324±0.0119	0.240±0.0219*
GPE	0.107±0.0172	0.0884±0.00930	0.121±0.0201	0.149±0.0166	0.104±0.00904	0.0968±0.00818

Metabolite µmol/g liver	Rat					
	72 h		120 h		168 h	
	C	T	C	T	C	T
DHAP	0.323±0.0233	0.417±0.0586	0.306±0.0297	0.360±0.0246	0.392±0.0537	0.332±0.0306
G3P	2.21±0.0822	2.52±0.278	2.45±0.148	2.30±0.116	2.48±0.116	2.45±0.136
G3P/DHAP	6.94±0.476	6.27±0.637	8.29±0.845	6.59±0.723	6.69±0.686	7.61±0.675
G6P	0.687±0.0721	0.691±0.0816	0.835±0.0795	0.594±0.0481*	0.686±0.0380	0.627±0.0417
Pcho	2.98±0.208	9.60±1.72*	3.06±0.287	8.41±0.587*	2.81±0.148	7.33±0.356*
Peth	0.485±0.0472	0.753±0.134	0.666±0.0437	0.532±0.0195*	0.756±0.130	0.516±0.0717
GPC	0.248±0.0210	0.260±0.0385	0.248±0.0376	0.241±0.0260	0.228±0.0159	0.254±0.0299
GPE	0.292±0.0281	0.307±0.0617	0.239±0.0353	0.250±0.0389	0.217±0.0479	0.256±0.0387

TABLE 15. Effect-derived differences in mean levels of specific hepatic metabolites measured by ^{31}P NMR spectroscopy of aqueous extracts (μmol/g liver) for treatment, species, and time. Also shown is the G3P/DHAP ratio. Statistical significance was determined as in Table 2. M=mouse, R=rat, T=treated, C=control, h=hours post-dose, NS=no significant difference detected, NA=not appropriate. The p-values are not adjusted for multiple testing

	Treatment (treated *vs.* control)			**Species (rat *vs.* mouse)**			**Time (72 h *vs.* 120 h *vs.* 168 h)**		
	Main Effect (M + R)	**M**	**R**	**Main Effect (T + C)**	**T**	**C**	**Main Effect (M + R)**	**M**	**R**
G3P	NS	NS	NS	NA	NA	NS	NA	120 h>168 h (p = 0.0031)	NS
G3P/DHAP	NS	NS	NS	M < R (p=0.0005)	NS	NS	NA	NS	NS
G6P	C > T (p=0.0066)	NS	NS	M > R (p=0.0019)	NS	NS	NS	NS	NS
Pcho	NA	NS	C < T 2.6-3.2-fold (p<0.0001)	NA	M < R 6.8-14.2-fold (p<0.0001)	M < R 2.8-3.8-fold (p<0.0001)	NS	NS	NS
GPC	NA	NS	NS	NA	NS	M > R 1.4-1.9-fold (p=0.0465)	NS	NS	NS
GPE	NS	NS	NS	M < R (p<0.0001)	NS	NS	NS	NS	NS

f. Effects of TCDD on the Mean Hepatic SphM/Pcho Ratio

Figure 20 shows how the mean SphM/Pcho ratio differs between mice and rats, across time. The three-factor ANOVA shows that the data in the whole model for the ratio is significant ($p<0.0001$). Species, time, and treatment together are significant ($p=0.0413$). At 72 hours, the mean ratio in TCDD-treated mice is 1.6-fold higher than that in control mice. The one-factor ANOVA shows that the ratio is significant only at 72 hours in mice ($p=0.0566$), and at all times in rats ($p=0.0009$, 0.0019, 0.0029). The ratio is *ca.* 76% lower in treated rats relative to control rats, at all times. There is also a significant time effect, in treated mice ($p=0.0005$) as well as in control ($p=0.0484$) and treated rats ($p=0.0369$).

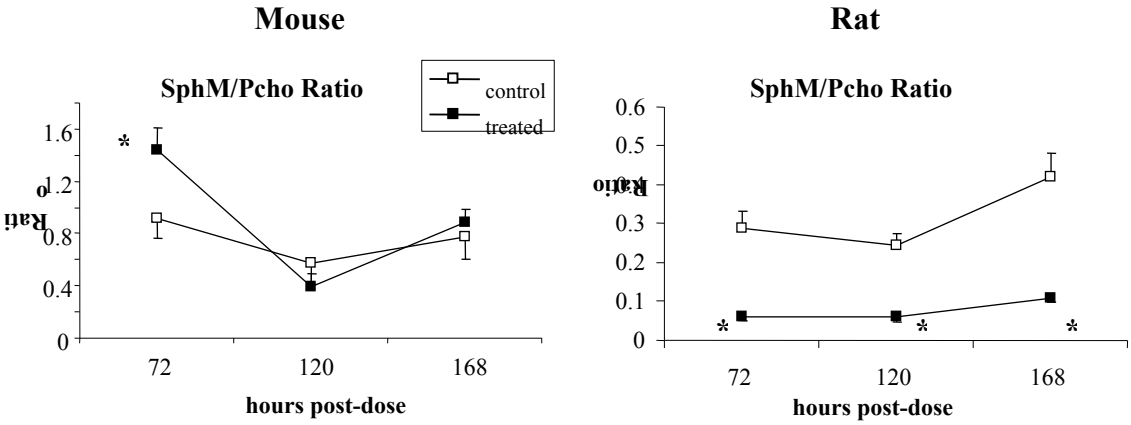

FIG. 20. TCDD-induced changes in the mean hepatic SphM/Pcho ratio in mice and rats over time (mean ± SE; *n*=3-5). Empty boxes represent vehicle controls, and filled boxes treated animals. Bars represent **±** standard error from the mean. The asterisk denotes a significant difference in treated *vs*. control mice and rats at the specified time ($p\leq0.05$).

Table 16 summarizes the mean SphM/Pcho ratio in TCDD-treated and vehicle control mice and rats at each of the three times post-dose.

TABLE 16. Mean SphM/Pcho ratio measured by NMR spectroscopy of liver and aqueous extracts from TCDD-treated and vehicle control mice and rats at 72, 120, and 168 hours post-dose (Mean ± SE; *n*=3-5 per group). The asterisk denotes significant differences ($p \leq 0.05$) between TCDD-treated and vehicle control animals at the specified time post-dose (one-factor ANOVA with post-hoc Tukey-Kramer Honestly Significant Difference). C=control, T=treated, h=hour.

Ratio	Mouse					
	72 h		120 h		168 h	
	C	T	C	T	C	T
SphM/Pcho	0.915 ± 0.154	1.44 ± 0.175*	0.574 ± 0.162	0.389 ± 0.100	0.777 ± 0.170	0.888 ± 0.0976

Ratio	Rat					
	72 h		120 h		168 h	
	C	T	C	T	C	T
SphM/Pcho	0.289 ± 0.0426	0.0613 ± 0.0121*	0.242 ± 0.0311	0.0622 ± 0.0138*	0.421 ± 0.0614	0.108 ± 0.0101*

3. Hepatic Metabolites Analyzed by ^{1}H NMR Spectroscopy of Aqueous Extracts

Levels of lactate and pyruvate are obtained from the ^{1}H NMR spectra. The analysis includes control mouse #32, since the ^{1}H NMR spectrum did not appear affected by the paramagnetic cations that remained in the sample. Peaks were identified using reported literature values, and chemical shifts, in ppm, are indicated in Table 17.

TABLE 17. Chemical shifts (on the ppm scale) of common hydrogen-functional groups observed in mouse and rat liver aqueous extracts in ^{1}H NMR spectra, referenced to TSP at 0.0 ppm. Bold denotes the specific hydrogen atom that the peak represents.

Chemical shift (ppm)	Molecule	Assignment
4.11	lactate	C**H**
1.33	lactate	C**H$_3$**
2.4	pyruvate	C**H$_3$**

Table 18 shows the saturation factors calculated when analyzing the ^{1}H NMR spectra of aqueous extracts.

TABLE 18. Saturation factors of specific aqueous metabolite signals analyzed by ^{1}H NMR spectroscopy. All values were expressed as a ratio of integrated intensity relative to TSP for ^{1}H NMR spectroscopy. FR=fully relaxed data, PS=partially saturated data, SF=saturation factor=FR/PS.

^{1}H metabolite	FR	PS	SF
Pyruvate	13.1	13.0	1.01
Lactate (4.11 ppm)	18.6	17.4	1.07
Lactate (1.33 ppm)	51.2	52.3	0.979

a. Effects of TCDD on Mean Hepatic Lactate and Pyruvate

1.) Hepatic Lactate

Figure 21 shows how mean hepatic lactate levels change in both rats and mice, across time post-dose. The data in the whole model is significant for mean lactate levels, by the three-factor ANOVA ($p<0.0001$). Species, time, and treatment together are significant ($p=0.0343$). In TCDD-treated mice, mean lactate levels significantly increase from 72 to 120 hours, and decrease from 120 to 168 hours.

Analysis of significant treatment effects using the one-factor ANOVA show that control and TCDD-treated mice exhibit significant changes only at 72 hours ($p=0.0004$).

At 72 hours, mean lactate levels in treated mice are 30% lower than that in control mice. Analysis of effects across time are significant in control and treated mice ($p=0.0056$, 0.0043). Rats exhibit no significant changes in mean lactate levels by either ANOVAs.

2.) Hepatic Pyruvate

The three-factor ANOVA shows the data in the whole model for mean levels of pyruvate is significant ($p<0.0001$). Time and species are significant ($p=0.0031$); however, changes across treatment are not ($p=0.2727$) (Figure 21). Mean pyruvate levels in mice significantly increase from 72 to 120 hours, and decrease from 120 to 168 hours. Mice and rats have significantly different mean levels at 72 and 120 hours. Mice at 120 hours have significantly higher mean levels than rats at 72 and 168 hours, but not at 120 hours. The one-factor ANOVA across treatment is not significant in either species; however, treated mice exhibit significant changes across time ($p=0.0142$).

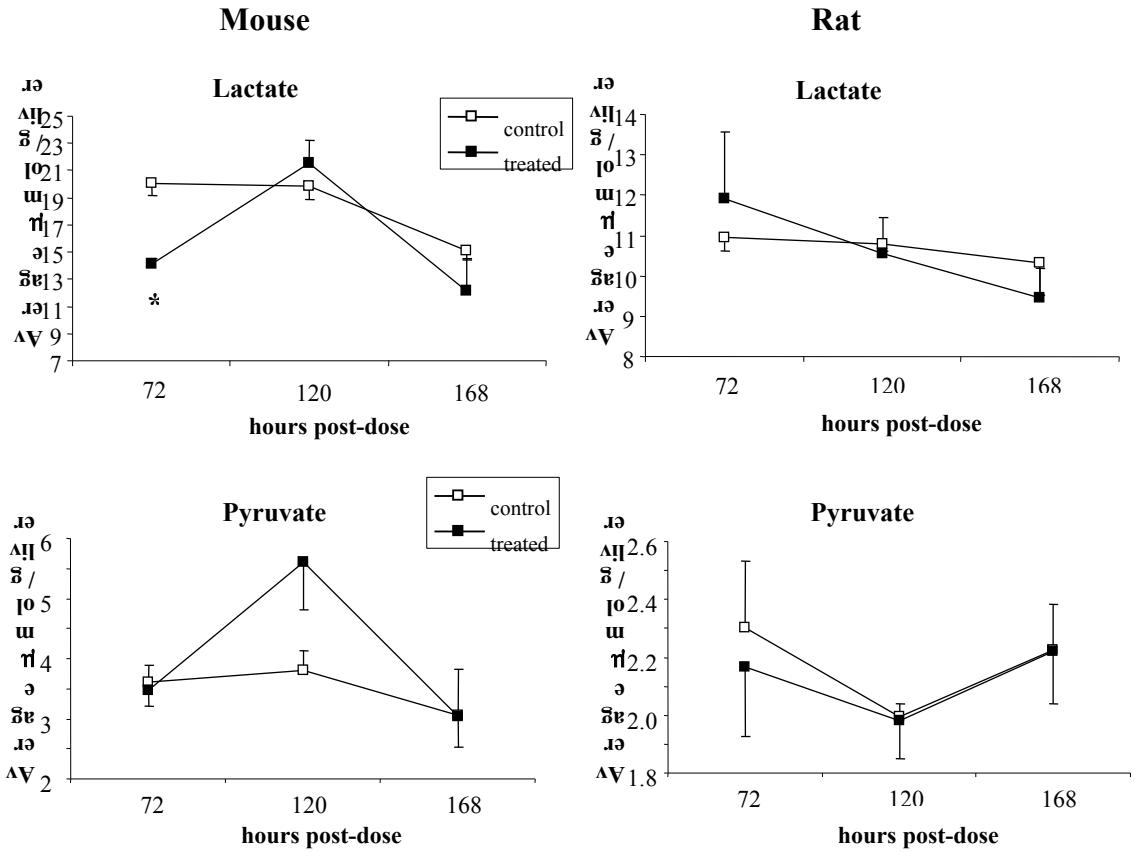

FIG. 21. Mean hepatic lactate and pyruvate levels (μmol/g liver; mean ± SE; *n*=4-5) measured by ^{1}H NMR spectroscopy in mice and rats as a function of time post-dose. Empty boxes represent vehicle controls, and filled boxes treated animals. Bars represent ± standard error from the mean. The asterisk denotes a significant difference in treated *vs*. control at the specified time ($p \leq 0.05$). See Table 20 for statistical differences across time.

b. Effects of TCDD on the Mean Hepatic Lactate/Pyruvate Ratio

Figure 22 shows how the lactate/pyruvate ratio changes across time, in both species. This ratio is another indicator of the cytosolic redox potential. When examining the mean ratio using the three-factor ANOVA, the data in the whole model is not significant (p=0.3082). According to mouse data in the figure, this does not make sense.

The one-factor ANOVAs did indeed find significant effects across treatment in mice. At 72 hours, the mean ratio in TCDD-treated mice is 26% lower than that in control mice (p=0.0053), and at 120 hours, it is 24% lower (p=0.0141). Mice do not

exhibit significant changes over time. The mean ratio is not significant across time or treatment in rats.

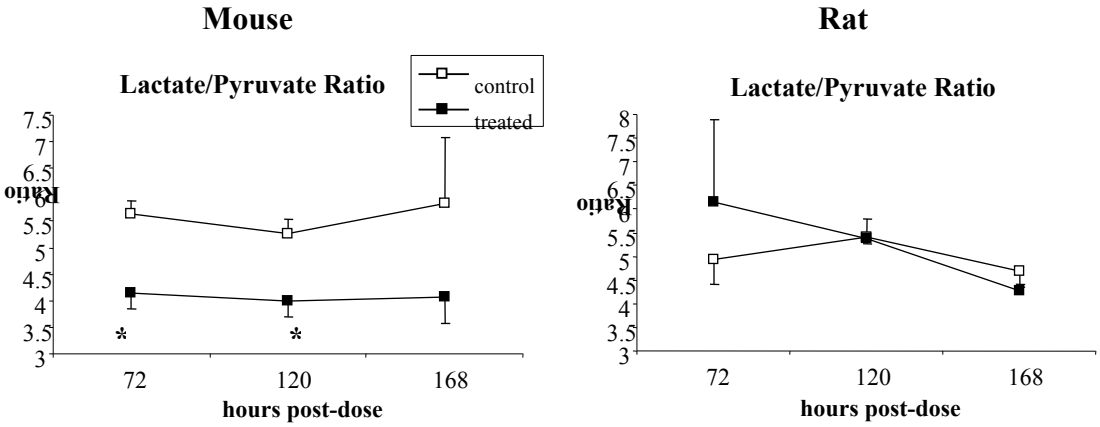

FIG. 22. TCDD-induced changes in the mean hepatic lactate/pyruvate ratio in mice and rats over time (mean ± SE; *n*=4-5). Bars represent ± standard error from the mean. The asterisk denotes a significant difference in treated *vs*. control at the specified time ($p \leq 0.05$). See Table 20 for statistical differences across time.

Summary of Metabolite Quantities Analyzed by ^{1}H NMR Spectroscopy of Aqueous Extracts

Table 19 summarizes metabolite quantities analyzed by ^{1}H NMR spectroscopy of the hepatic aqueous extracts. These quantities, in μmol/g liver, are mean levels obtained at each time post-dose and between treatment groups. Mean levels in treated and vehicle control rats and mice can be compared directly from this table. Table 20 shows the significant differences across time, in mean levels of these metabolites.

TABLE 19. Mean levels of hepatic metabolites measured by ^{1}H NMR spectroscopy of aqueous extracts from TCDD-treated and vehicle control mice and rats at 72, 120, and 168 hours post-dose (Mean ± SE; µmol/g liver; *n*=3-5 per group). Also shown is the lactate/pyruvate ratio for mice and rats. The asterisk denotes significant differences (p≤0.05) between TCDD-treated and vehicle control animals at the specified time post-dose (one-factor ANOVA with post-hoc Tukey-Kramer HSD). C=control, T=treated, h=hour.

Metabolite µmol/g liver	Mouse					
	72 h		120 h		168 h	
	C	T	C	T	C	T
Lactate	20.1±0.946	14.1±0.409*	19.8±0.988	21.5±1.66	15.1±0.695	12.2±2.31
Pyruvate	3.61±0.292	3.46±0.257	3.81±0.314	5.60±0.781	3.06±0.771	3.03±0.493
Lactate/Pyruvate	5.63±0.252	4.14±0.301*	5.26±0.270	3.98±0.277*	5.84±1.23	4.07±0.510

Metabolite µmol/g liver	Rat					
	72 h		120 h		168 h	
	C	T	C	T	C	T
Lactate	11.0±0.360	11.9±1.67	10.8±0.167	10.5±0.908	10.3±0.807	9.46±0.729
Pyruvate	2.30±0.229	2.17±0.238	2.00±0.0441	1.98±0.130	2.22±0.161	2.22±0.179
Lactate/Pyruvate	4.94±0.519	6.14±1.74	5.41±0.131	5.36±0.438	4.68±0.343	4.27±0.128

TABLE 20. Effect-derived differences in mean levels of specific hepatic metabolites measured by ^{1}H NMR spectroscopy of aqueous extracts (µmol/g liver) for treatment, species, and time. Statistical significance was determined as in Table 2. Lactate showed significant differences between treatment, time, and species (see results). The whole-factor ANOVA was not significant for pyruvate levels, but the two-factor ANOVA showed significant changes occurring (see results). M=mouse, R=rat, T=treated, C=control, h=hours post-dose, NS=no significant difference detected, NA=not appropriate. The p-values are not adjusted for multiple testing.

	Treatment (treated *vs.* control)			Species (mouse *vs.* rat.)			Time (72 h *vs.* 120 h *vs.* 168 h)		
	Main Effect (M + R)	M	R	Main Effect (T + C)	T	C	Main Effect (M + R)	M	R
Pyruvate	NS	NS	NS	NA	NS	NS	NA	72 h<120 h 120 h>168 h (p=0.0031)	NS

IV. DISCUSSION

This report will elucidate the different metabolic pathways affected by TCDD in mice and rats. Our NMR study of hepatic lipids (TAG, cholesterol, and *n*3 and *n*6 FAs) showed increased levels in mice but not rats, consistent with PCA results showing separation between control and treated mice, and overlapping clusters in rats. The following sections will discuss four possible pathways affected by TCDD: A) increased TAG synthesis in mice, B) increased cholesterol uptake in mice, C) activation of sphingomyelinase in rats, and D) mitochondrial damage in both mice and rats. Comparisons will be made between these pathways and genomic effects.

A. Increased Levels of Hepatic TAG Suggest TAG Synthesis is Upregulated in Mice

NMR spectroscopy analyses show that mean hepatic levels of TAGs increased two to three-folds at all times in TCDD-treated mice (Figure 5). These increased levels may be explained by upregulated TAG synthesis. TAGs are synthesized from FAs and G3P. FAs esterified with CoA are condensed with the glycerol moiety of G3P to form phosphatidic acid (PA). G3P can be derived from glucose or glycerol or other three-carbon compounds that are used for gluconeogenesis. Loss of the phosphate group via PA phosphohydrolase yields DAG. Transfer of another FA acyl-CoA to the glycerol backbone, via DAG acyltransferase, yields TAG. DAG kinase catalyzes the reverse step of PA phosphohydrolase.

If TAG synthesis is upregulated in TCDD-treated mice, and G3P is utilized for TAG synthesis, the G3P-dehydrogenase reaction (a NAD^+/NADH-linked dehydrogenase, Figure 23) will favor the production of G3P. This is supported by the finding that DHAP levels decreased 49% in TCDD-treated mice (Figure 15). This decrease in DHAP in treated mice may be due to utilization of G3P for TAG synthesis.

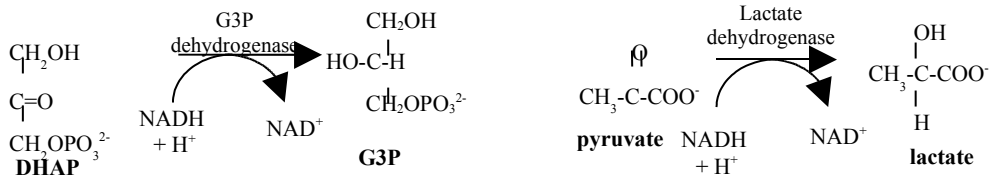

FIG. 23. G3P and lactate dehydrogenase reactions

However, the G3P/DHAP ratio only shows a significant species difference. The ratio is higher in mice than rats (Figure 16). The shift in the G3P-dehydrogenase equilibrium causes a shift in the cytosolic redox potential, decreasing the NADH/NAD^+ ratio. Since the lactate-dehydrogenase reaction operates near equilibrium and depends on this redox potential, this change in the NADH/NAD^+ ratio will drive the lactate-dehydrogenase reaction towards production of pyruvate. This, in turn, will cause the lactate/pyruvate ratio to decrease. Indeed, in mice treated with TCDD, the lactate/pyruvate ratio significantly decreased *ca.* 25% at 72 and 120 hours (Figure 22). Rats showed no significant changes in the lactate/pyruvate ratio. Thus, there may be a driving force to synthesize G3P for TAG synthesis in treated mice (Figure 24).

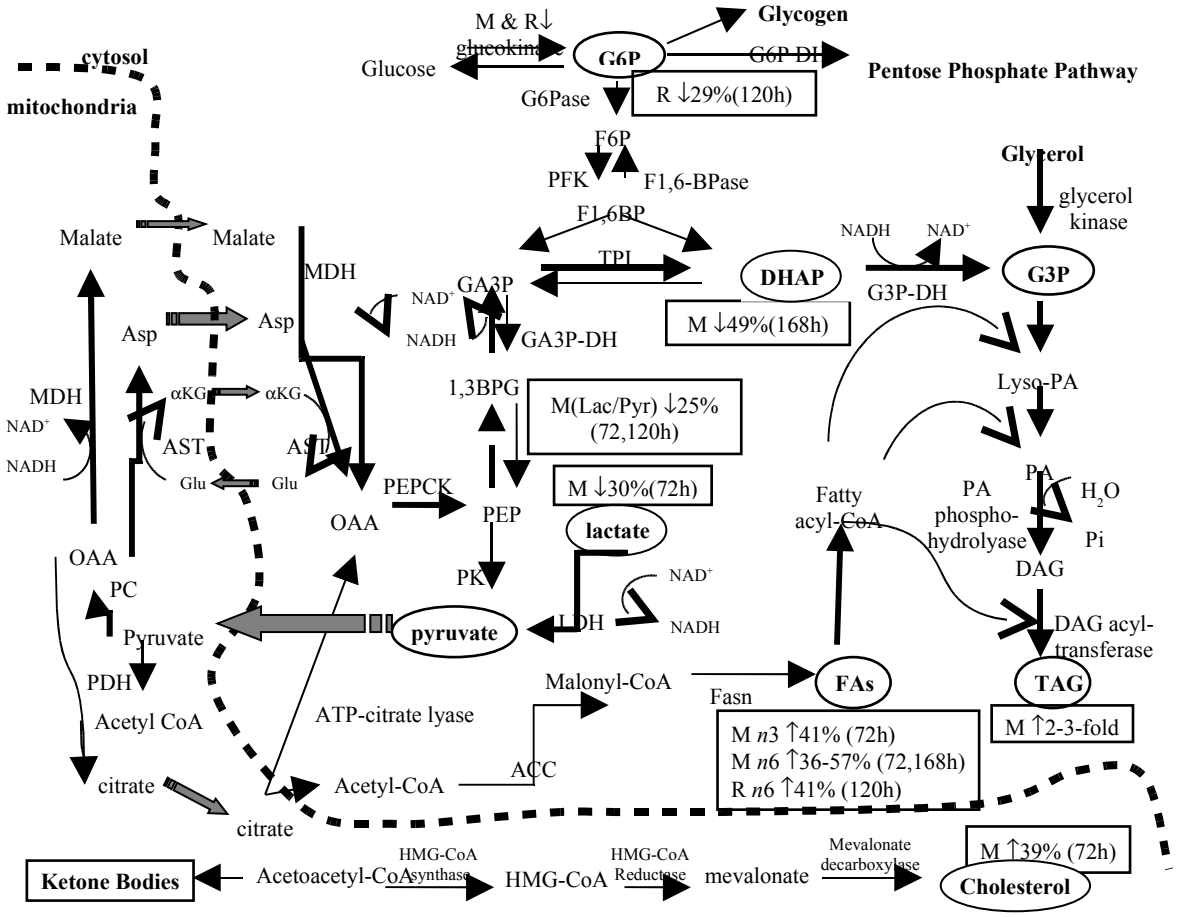

FIG. 24. Gluconeogenesis, TAG synthesis, and Cholesterol Synthesis in TCDD-Treated Mice and Rats. Metabolites circled were measured by NMR spectroscopy. A rectangle box placed adjacent to a metabolite indicates a statistically significant difference in the level of this metabolite (treated *vs*. control; $p \leq 0.05$). Information in this box designates: (1) the species that showed change (M=mouse; R=rat), (2) whether the metabolite increased or decreased (up or down arrow), (3) the magnitude of change (% relative to control), and (4) the designated time-point (h=hour). Bold arrows indicate pathways possibly upregulated in response to TCDD. Heavy gray arrows show transport of metabolites between the cytosol and mitochondrion. The dashed line represents the inner mitochondrial membrane. Abbreviations: 1,3BPG, 1,3-bisphosphoglycerate; ACC, acetyl-CoA carboxylase; αKG, α–ketoglutarate; Asp, aspartate; AST, aspartate aminotransferase; CoA, coenzyme A; DAG, diacylglycerol; DAG acyltransferase, diacylglycerol acyltransferase; DAG kinase, diacylglycerol kinase; DHAP, dihydroxyacetone phosphate; F1,6BP, fructose-1,6-bisphosphate; F1,6-BPase, fructose-1,6-bisphosphatase; F6P, fructose-6-phosphate; FA, fatty acid; Fasn, fatty acid synthase; G3P, glycerol-3-phosphate; G3P-DH, glycerol-3-phosphate dehydrogenase; G6P, glucose-6-phosphate; G6P DH, glucose-6-phosphate dehydrogenase; GA3P, glyceraldehyde-3-phosphate; GA3P DH, glyceraldehyde-3-phosphate dehydrogenase; Glu, glutamate; HMG-CoA, hydroxymethylglutaryl CoA; Lac/Pyr, lactate/pyruvate ratio; LDH, lactate dehydrogenase; Lyso-PA, lysophosphatidic acid; MDH, malate dehydrogenase; NAD^+, nicotinamide adenine dinucleotide; NADH, reduced nicotinamide adenine dinucleotide OAA, oxaloacetate; PA, phosphatidic acid; PA phosphohydrolase, phosphatidic acid phosphohydrolase; PC, pyruvate carboxylase; PDH, pyruvate dehydrogenase; PFK, phosphofructokinase; PEP, phosphoenolpyruvate; PEPCK, phosphoenolpyruvate carboxykinase; PK, pyruvate kinase; TAG, triacylglyceride; TPI, triose phosphate isomerase.

Another measure of the cytosolic redox potential can come from the glyceraldehyde-3-phosphate dehydrogenase reaction. Neither glyceraldehyde-3-phosphate nor 1,3-bisphosphoglycerate were measured, but will be done in the future, from the ^{31}P NMR spectra.

NMR spectroscopy analyses of hepatic G6P show G6P levels were not affected in TCDD-treated mice. This is consistent with the hypothesized mechanism that gluconeogenesis may be occurring to the level of the trioses, and to TAG synthesis. In TCDD-treated rats at 120 hours, levels significantly decreased (by 29%) relative to vehicle controls (Figure 17). This decrease in rats may be explained by inhibited gluconeogenesis. Another possibility is the pentose phosphate pathway. Reductive biosynthesis may be occurring, suggesting a need for NADPH for reducing power.

TAG Synthesis in Mice – Comparison to Genomic Effects

Work is ongoing to examine mRNA expression or activities of enzymes in the TAG synthetic pathway from G3P (PA phosphohydrolase, DAG acyltransferase, and DAG kinase), to confirm the upregulation of TAG synthesis in mice. PA phosphohydrolase activity is known to be increased by FAs. Hepatic levels of FAs are elevated in TCDD-treated mice, so it is expected that the activity of this enzyme would be upregulated and TAG synthesis is active.

Reports show that the mRNA expression of glucokinase, the enzyme that converts glucose to G6P, is inhibited by TCDD in mice and rats (Boverhof *et al*., 2005; Fletcher *et al.*, 2005). However, its repression in mice occurs at 12 and 24 hours, earlier time-points than those observed in this study. Fletcher and coworkers used male Sprague-Dawley rats, administered 40 μg/kg body weight, and reported that the downregulation of

glucokinase could explain the altered glucose production and decreased G6P levels in TCDD-treated rat liver (Fletcher *et al*., 2005). It would be interesting to see what happens to messenger levels of this enzyme in mice treated with TCDD, from 72 to 168 hours.

The activity of G3P dehydrogenase may be affected in a way that favors the synthesis or buildup of G3P, and thus TAG levels in mice. Also, phosphoenolpyruvate carboxykinase might be upregulated. This enzyme is the rate-limiting step in gluconeogenesis from lactate and pyruvate. However, it is downregulated in mice, at 18 and 24 hours, earlier time-points than observed in this study (Boverhof *et al.*, 2005, 2006). Again, information into what happens at the time-points examined in our study could be valuable. Also, alanine, glutamate, and aspartate levels will be quantified from ^{1}H NMR spectra of aqueous extracts as future work.

TCDD-Induces Fatty Acid Uptake and Metabolism

NMR spectroscopy analyses show significant increases in mean hepatic levels of *n*3 and *n*6 FAs with TCDD treatment in mice (Figure 6). Increased levels of FAs may indicate upregulated FA synthesis. In de novo FA synthesis, the products of glycolysis are converted to FAs. Pyruvate carboxylase releases oxaloacetate, which goes into the Krebs Cycle (TCA) to form citrate. Citrate is then transported to the cytosol where it is broken down to oxaloacetate and acetyl-CoA by ATP-citrate lyase. Acetyl-CoA is carboxylated to malonyl-CoA, and FA synthase produces palmitate. However, palmitate does not synthesize *n*3 or *n*6 FAs. Instead, the increased levels of FAs in mice may be explained by FA uptake. Examination into the serum free FA levels support increased FA mobilization from adipose tissue to the blood to liver. Zacharewski and coworkers

found, using the same strains of female i.o. rodents as our study, that serum free FA significantly increased *ca.* 22% in TCDD-treated mice from 72 to 168 hours ($p<0.05$) (Boverhof *et al*., 2006). This hypothesis is supported by histopathology and microarray data. H*epatic tissue in mice revealed vacuolization due to TAG or FA accumulation* (Boverhof *et al*., 2006), *consistent with reported gene expression findings that mediate increased uptake in mouse. Such gene findings include upregulation of Cd36 antigen (3.4-fold at 168 hours), lipoprotein lipase (3.5-fold at 168 hours), Lipin2 (3-fold at 72 hours), and very low-density lipoprotein receptor (1.8-fold at 72 hours). Null mutations of Cd36 antigen result in reduced FA uptake, and overexpression increases FA uptake and metabolism (Bonen et al., 2004; Febbraio et al., 1999). Lipoprotein lipase is involved in TAG metabolism and lipoprotein uptake (Weinstock et al., 1995).* Lipin2, when deficient, prevents normal lipid accumulation (Peterfy *et al*., 2001). *Very low-density lipoprotein receptor mediates the degradation of TAG-rich lipoproteins (Yagyu et al., 2002). The regulation of these genes may lead to the increased uptake and accumulation of TAG and FA in liver.*

The mRNA expression of ATP-citrate lyase in mice remains to be determined. Reports have shown that ATP-citrate lyase inhibitors decrease the syntheses of FA and cholesterol (Pearce *et al*., 1998; Sullivan *et al*., 1974). *It would be interesting to look into messenger levels of pyruvate carboxylase in mice as well.*

B. Increased Levels of Hepatic Cholesterol Suggests Cholesterol Uptake in Mice

This report shows that mean hepatic cholesterol levels significantly increased 21-39% in TCDD-treated mice relative to control. Treated *vs*. control rats show no significant differences (Figure 5). This finding may suggest increased cholesterol

synthesis or an increase in the uptake of cholesterol into liver, in treated mice. In de novo synthesis, acetyl-CoA is first converted to mevalonate via acetoacetyl-CoA synthase, hydroxymethylglutaryl-CoA (HMG-CoA) synthase, and HMG-CoA reductase. An isoprene unit is formed from mevalonate via mevalonate decarboxylase. Squalene then becomes cholesterol (Figure 24).

Interestingly, only mice exhibit significant alterations in serum cholesterol, decreasing *ca.* 30% at 72 to 168 hours ($p<0.05$) (Boverhof *et al.,* 2006). The finding that serum cholesterol decreased and hepatic cholesterol increased by similar amounts, suggests that the uptake of cholesterol to liver might be occurring in mice.

Cholesterol Uptake in Mice – Comparison to Genomic Effects

In mice, mRNA expression for low density lipoprotein receptor-related protein was upregulated by three-fold at 72 to 168 hours (Boverhof *et al*., 2005). The upregulation of this protein may explain the increased levels of hepatic cholesterol and reduced serum levels. To confirm the hypothesis that cholesterol uptake is occurring in mice, it would be interesting to examine mRNA expression of HMG-CoA synthase and reductase (rate-limiting step) in mouse. Also, levels of mevalonate can be quantified from the ^{1}H NMR spectra.

C. Activation of Sphingomyelinase in Rats

In TCDD-treated rats, mean hepatic SphM levels are 30-38% lower than controls at 72 and 168 hours, and not significantly changed in mice (Figure 12). SphM is a phospholipid involved in development and differentiation, the cellular response to cytokines, and apoptosis (Dressler *et al*., 1992; Hannun 1994, 1996; Hannun and Obeid,

1995; Obeid and Hannun, 1995). TCDD-treated rats have significantly higher levels of Pcho (*ca.* three-fold relative to control) (Figure 18).

The activation of sphingomyelinase results in a buildup of Pcho and ceramide, and the SphM and Pcho data in rats are consistent with this pathway (Figure 25). SphM turnover to ceramide mediates the cellular response to tumor necrosis factor (TNF-α). The decreased SphM/Pcho ratio in treated rats at all times suggests that TCDD induces the activation of sphingomyelinase, possibly through TNF-α (Figure 20). Also interesting are the findings that the SphM/Pcho ratio increase and levels of lactate decrease at 72 hours post-dose in TCDD-treated mice relative to controls. It has been reported that, in primary Sertoli cell cultures, TNF-α stimulates lactate dehydrogenase (isoform A) expression and activity through the SphM hydrolysis pathway (more specifically, via sphingosine production) (Grataroli *et al*., 2000).

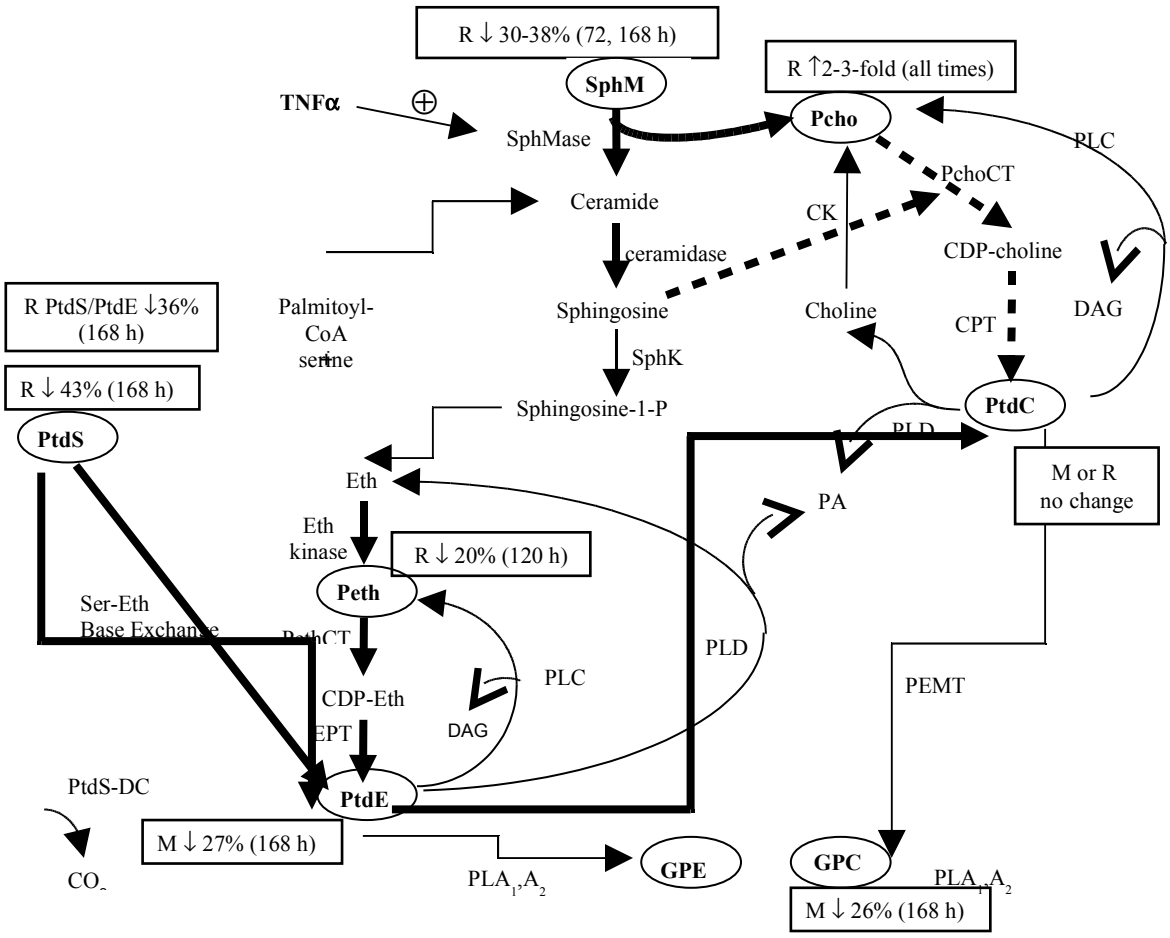

FIG. 25. **Sphingomyelin Pathway in TCDD-Treated Mice and Rats.** Metabolites circled were measured by NMR spectroscopy. A rectangle box placed adjacent to a metabolite indicates a statistically significant difference in the level of this metabolite (treated *vs*. control; $p \leq 0.05$). Information in this box designates: (1) the species that showed change (M=mouse; R=rat), (2) whether the metabolite increased or decreased (up or down arrow), (3) the magnitude of change (% relative to control), and (4) the designated time-point (h=hour). Bold arrows indicate pathways that are activated, dashed arrows indicate pathways that are inhibited. Abbreviations: CDP-Eth, CDP ethanolamine, CK, choline kinase; CPT, choline phosphotransferase; DAG, diacylglycerol; EK, ethanolamine kinase; EPT, ethanolamine phosphotransferase; Eth, ethanolamine; Ser-Eth base exchange, serine-ethanolamine base exchange; GPC, glycerophosphocholine; GPE, glycerophosphoethanolamine; PA, phosphatidic acid; Pcho, phosphocholine; PchoCT, phosphocholine-CDP cytidyltransferase; PEMT, phosphatidylethanolamine methyltransferase; Peth, phosphoethanolamine; Peth-CT, phosphoethanolamine-CDP cytidyltransferase; PLC, phospholipase-C; PLD, phospholipase-D; PLA_1, phospholipase-A_1, PLA_2, phospholipase-A_2; PtdC, phosphatidylcholine; PtdE, phosphatidylethanolamine; PtdS, phosphatidylserine; PtdS DC, PtdS decarboxylase; SphK, sphingosine kinase; SphM, sphingomyelin; SphMase, sphingomyelinase; TNF-α, tumor necrosis factor-α.

Pcho can also be utilized in de novo PtdC synthesis (Figure 25). Pcho is first converted to CDP-choline (via Pcho-CDP cytidyltransferase) and then to PtdC (via CDP-choline:1,2-DAG cholinephosphotransferase). The NMR spectroscopy analyses show that TCDD did not affect PtdC levels in either mice or rats (Figure 9). The following step in the SphM pathway may account for PtdC levels not being affected by TCDD. The next step in SphM turnover is the hydrolysis of ceramide to sphingosine, and sphingosine is a potent inhibitor of Pcho-CDP cytidyltransferase (Merrill 1989; Sohal and Cornell, 1990). This cytidyltransferase is the rate-limiting enzyme in de novo PtdC synthesis from Pcho. Thus, the regulation of de novo synthesis of PtdC is affected by TCDD in rats, to the level of CDP-choline. The activation of sphingomyelinase and inhibition of Pcho-CDP cytidyltransferase are consistent with the large increase in Pcho.

SphM metabolism continues with the phosphorylation of sphingosine to sphingosine-1-phosphate, by sphingosine kinase (Figure 25). Sphingosine-1-phosphate can be dephosphorylated or cleaved to 1) Peth and trans-2-hexadecenal from sphingosine or 2) palmitaldehyde from sphinganine. The aldehyde intermediate can be oxidized to FAs.

Another source of PtdC is from PtdE, via PtdE-N-methyltransferase (Figure 25). However, mean PtdE levels did not significantly change in rats (Figure 9). PtdE synthesis is then upregulated via the Kennedy pathway (via Peth-CDP cytidyltransferase), and from PtdS via 1) serine-ethanolamine base exchange or 2) PtdS decarboxylase. Thus, Peth and PtdS are both precursors to PtdE (Figure 25). Mean hepatic levels of PtdS decrease by 43% with TCDD treatment in rats at 168 hours post-dose (Figure 8). Peth is also decreased due to utilization in the Kennedy pathway. Also,

the PtdS/PtdE ratio decreased 36% at 168 hours in rats (Figure 11), suggesting that PtdE is synthesized from PtdS. However, it is not known whether this synthesis is via base-exchange or decarboxylation. Levels of serine and ethanolamine will be measured from the ^{1}H NMR spectra in the near future to determine if TCDD affects the serine-ethanolamine base-exchange reaction. It would also be interesting to compare Peth and PtdE levels to determine if PtdE is being synthesized from Peth instead of PtdS.

Interestingly, the PtdC/PtdE ratio changed to a similar extent in both rats (12-22% increase at all times) and mice (17-23% increase at 72 and 120 hours) (Figure 10). This suggests that this phospholipid pathway is also affected in TCDD-treated mice. This is corroborated by Pcho and SphM findings. Although mean hepatic levels of these metabolites do not show significant treatment effects (Figures 12 and 18), there is a transient effect, whereby a decrease in SphM is accompanied by an increase in Pcho at the same time points.

Metabolites affected in the general phospholipid pathway in TCDD-treated mice include GPC and PtdE. GPC levels are 26% lower in treated mice relative to control mice (Figure 19). PtdE levels decrease 27% at 168 hours (Figure 9). PtdC can be converted to GPC and PtdE to GPE by phospholipases (Figure 25).

The first step in de novo synthesis of SphM is the condensation of palmitoyl-CoA and serine. Serine loses its carboxyl group via serine palmitoyltransferase to produce 3-ketosphinganine. 3-ketosphinganine is reduced to form sphinganine. Sphinganine is acylated to dihydroceramides by ceramide synthase, and SphM is produced from ceramide. SphM can also be synthesized by the PtdC-mediated transfer of Pcho to ceramide, at the same time releasing DAG, which is a precursor to TAG. PtdC might be

degraded for the synthesis of SphM, which releases DAG to form TAG. This is consistent with TAG results observed in mice (Figure 5). Choline levels could be examined to corroborate this hypothesis. PtdC synthesizes choline, and choline kinase converts choline to Pcho (Figure 25).

Several groups reported that TCDD enhances the inflammatory response (Clark *et al*., 1991; Katz *et al*., 1984; Sutter *et al*., 1991). This is consistent with liver histopathology: inflammatory cells were manifested in TCDD-treated mice (Boverhof *et al*., 2005). Also, Fan and his group used liver sections from TCDD-treated rats, and found that TCDD is capable of increasing the level of TNF-α. They observed that at 30 μg/kg TCDD, mRNA levels of TNF-α are greatly increased (Fan *et al.*, 1997). Also, the AhR has a role in the inflammatory response to TCDD. Thurmond and his coworkers reported that, in TCDD-treated animals lacking the AhR in hematopoietic cells, there is almost no inflammatory response (Thurmond *et al.*, 1999).

Sphingomyelin Pathway – Comparison to Genomic Effects

Studies by our group and others found upregulation in gene expression for TNF-α and the receptor with TCDD treatment (Fletcher *et al*., 2005; Kerkvliet 1995; Lee *et al*., 2004, Thurmond *et al*., 1999). This supports our TNF-α hypothesis. Also, the mRNA expression for sphingosine kinase is upregulated 1.7-fold in rats, supporting TNF-α-induced activation of sphingomyelinase. However, this induction occurs at 4 hours, a time-point not examined in our study (Boverhof *et al*., 2006). We are currently looking into measures of TNF-α and mRNA expression from 72 to 168 hours in rats. In rats, the activity of PtdE-N-methyltransferase is downregulated 0.4-fold at 168 hours (Boverhof *et al*., 2006). While this is not consistent with our NMR spectroscopy findings into PtdC

and PtdE levels, a feedback inhibition mechanism may be occurring. In such a mechanism, the activity of PtdE-N-methyltransferase might be upregulated and gene expression downregulated.

D. TCDD Induces Oxidative Stress in both Rats and Mice

This study shows that mean hepatic levels of cardiolipin decreased by *ca.* 20% in both rats and mice at 168 hours (Figure 8). Cardiolipin is almost exclusively localized in the inner mitochondrial membrane. Cardiolipin and its oxidation products are important signaling molecules in apoptosis (Kagan *et al*., 2004, 2006, 2008). Cardiolipin oxidation is required for release of pro-apoptotic factors from mitochondria into cytosol. Early in apoptosis, massive amounts of cardiolipin translocate the outer mitochondrial membrane, and are available to interact with cytochrome c. Cytochrome c is a cardiolipin-specific peroxidase that controls energy metabolism in the electron transport chain shuttle. Cytochrome c/cardiolipin complexes are formed, which then generate cardiolipin hydroperoxides, or reactive oxygen species (ROS). ROS production leads to oxidative stress, lipid peroxidation (Stohs 1990), and DNA damage (Shertzer *et al*., 1998; Wahba *et al*., 1988). It is hypothesized that cardiolipin levels decreasing to a similar extent at the same time-point in mice and rats may be indicative of mitochondrial damage or ROS production.

One study reported that mitochondria play a role in TCDD-elicited oxidative stress (Senft *et al*., 2002a), based on decreases in ATP, cytochrome oxidase, and aconitase activity. The decreased aconitase activity results in increased levels of superoxide, and thus ROS. Glutathione peroxidase, glutathione reductase, and thiol levels are increased. Mitochondrial damage and oxidative stress in rodents treated with

TCDD have been reported. In TCDD-treated rats, signs of oxidative changes include increased lipid peroxidation and decreased membrane fluidity (Stohs *et al.,* 1989). In livers of C57BL/6 mice, oxidative stress is characterized by increases in oxidized to reduced glutathione (GSSG/GSH) (Shertzer *et al.*, 1998). The decreased membrane fluidity is consistent with increased cholesterol uptake in TCDD-treated mice. The structure of cholesterol plays a role in maintaining the fluidity of cell membranes. Cholesterol has a rigid ring system and a short branched hydrocarbon tail, which interferes with close packing of FA tails. The high levels of cholesterol in TCDD-treated mice may be the cause of the decreased membrane fluidity. Thus, the literature has shown TCDD causes oxidative stress in mice and rats, and is supported by our cholesterol data.

Oxidative Stress – Comparison to Genomic Effects

Reports have shown that TCDD induces genes associated with the response to chemical stress and xenobiotic metabolism. Members of the AhR gene battery are induced by TCDD. The AhR gene battery includes Cyp1a1, NAD(P)H dehydrogenase, and xanthine dehydrogenase. TCDD also induces increases in glutathione transferases. The induction of glutathione transferases catalyzes the conjugation of reduced glutathione to products of oxidative stress (Raza *et al.,* 2002). ROS formation by TCDD depletes GSH levels, leaving cells susceptible to oxidative damage. Such GSH-synthesizing enzymes are glutamate-cysteine ligase (1st and rate-limiting step) and glutathione synthase (2nd step), both of which are induced by TCDD. Another gene induced by TCDD is UDP-glucose dehydrogenase. This dehydrogenase catalyzes the step going from UDP-glucose to UDP glucuronic acid, which is then conjugated to reactive

xenobiotics. Their induction serves an important role in detoxification, but may also contribute to ROS formation, leading to cellular oxidative stress and DNA fragmentation (Barouki and Morel, 2001; Boverhof *et al*., 2005).

The AhR plays a role in ROS production. Senft and coworkers found that TCDD-induced ROS was dependent on the AhR in female mice, but independent of CYP1A1 and CYP1A2 (Senft *et al.,* 2002b). Using AhR, CYP1A1, and CYP1A2(-/-) knockout mice, only AhR(-/-) mice were protected from TCDD-induced production of mitochondrial ROS and an oxidative stress response.

Future work will continue to probe into this oxidative damage hypothesis. Levels of choline and betaine will be measured from ^{1}H NMR spectra of aqueous extracts. Choline is a precursor to betaine, a hepatic osmolyte that protects against the development of steatosis (Patrick 2002). It is also involved in ischemia/reperfusion injury, possibly by the inhibition of Kupfer cell activation (Wettstein *et al.*, 1997). Betaine may be involved in steatosis and mitochondrial damage. Also, glutathione levels will be examined. It was not possible to identify, for certain, which peaks were the cysteine, glycine, and glutamate moieties of glutathione due to the overlap of multiple peaks in the spectrum. Total Correlation Spectroscopy (TOCSY) will be performed in the near future to resolve this problem.

V. CONCLUSIONS

Female i.o. C57BL/6 mice treated with TCDD exhibit steatosis, but not Sprague-Dawley rats, based on liver lipid content, PCA, and metabolic data from NMR spectroscopy. Liver lipid content significantly increased in TCDD-treated mice but not rats. PCA of lipids using ^{13}C NMR spectroscopy showed separation between control and treated mice but not rats. Consistent with these findings, mice show increases in TAG, cholesterol, and *n*3 and *n*6 FAs. Lipid accumulation in mice can be due to increased hepatic TAG synthesis, FA mobilization from adipose tissue to liver, and increased cholesterol uptake. In mice, liver aqueous extracts revealed decreases in the lactate/pyruvate ratio and DHAP levels. These findings are consistent with the decreased cytosolic NADH/NAD^+ ratio and upregulated TAG synthesis. TCDD-treated rats exhibited *ca.* 34% lower levels of hepatic SphM, and three-folds higher Pcho levels, suggestive of sphingomyelinase activation by TCDD, perhaps by TNF-α. Decreased cardiolipin at 168 hours in both rats and mice may indicate that TCDD causes mitochondrial damage, or ROS production. These observations are consistent with hepatic histopathology and clinical chemistry, and support the hypothesis that TCDD elicits species-specific AhR-mediated effects. Further work into gene expression at the tested times post-dose in both rats and mice is needed to corroborate these metabolic pathways.

VI. REFERENCES

Abbott, B.D., Schmid, J.E., Pitt, J.A., Buckalew, A.R., Wood, C.R., Held, G.A., and Diliberto, J.J. (1999). Adverse reproductive outcomes in the transgenic Ah receptor-deficient mouse. *Toxicol. Appl. Pharmacol.* **155**, 62–70.

Adinehzadeh, M., and Reo, N.V. (1998). Effects of peroxisome proliferators on rat liver phospholipids: Sphingomyelin degradation may be involved in hepatotoxic mechanism of perfluorodecanoic acid. *Chem. Res. Toxicol.* **11**, 428-440.

Barouki, R., and Morel, Y. (2001). Repression of cytochrome P450 1A1 gene expression by oxidative stress: mechanisms and biological implications. *Biochem. Pharmacol*. **61**, 511–516.

Bertazzi, P.A., Bernucci, I., Brambilla, G., Consonni, D., and Pesatori, A.C. (1998). The Seveso studies on early and long-term effects of dioxin exposure: a review. *Environ. Health Perspect*. **106**, 625-633.

Bickel, M.H. (1982). Polychlorinated persistent compounds. *Experientia* **38**, 879-882.

Birnbaum, L.S. and Fenton, S.E. (2003). Cancer and developmental exposure to endocrine disruptors. *Environ.Health Perspect.* **111**, 389–394.

Bonen, A., Campbell, S.E., Benton, C.R., Chabowski, A., Coort, S.L., Han, X.X., Koonen, D.P., Glatz, J.F., and Luiken, J.J. (2004). Regulation of fatty acid transport by fatty acid translocase/CD36. Proc. Nutr. Soc. **63**, 245-249.

Boverhof, D.R., Burgoon, L.D., Tashiro, C., Chittim, B., Harkema, J.R., Jump, D.B., and Zacharewski, T.R. (2005). Temporal and dose-dependent hepatic gene expression patterns in mice provide new insights into TCDD-mediated hepatotoxicity. *Toxicol Sci*. **85**, 1048-1063.

Boverhof, D.R., Burgoon, L.D., Tashiro, C., Sharratt, B., Chittim, B., Harkema, J.R., Mendrick, D.L., and Zacharewski, T.R. (2006). Comparative toxicogenomic analysis of the hepatotoxic effects of TCDD in Sprague Dawley rats and C57BL/6 mice. Toxicol. Sci. **94,** 398-416.

Clark, G.C., Taylor, M.J., Tritscher, A.M., and Lucier, G.W. (1991). Tumor necrosis factor involvement in 2,3,7,8-tetrachlorodibenzo-*p*-dioxin-mediated endotoxin hypersensitivity in C57BL/6J mice congenic at the Ah locus. *Toxicol. Appl. Pharmacol.* **111,** 422–431.

Cranmer, M., Louie, S., Kennedy, R.H., Kern, P.A., and Fonseca, V.A. (2000). Exposure to 2,3,7,8-tetrachlorodibenzo-*p*-dioxin (TCDD) is associated with hyperinsulinemia and insulin resistance. *Toxicol. Sci*. **56**, 431–436.

Denison, M.S., Vella, L.M., and Okey, A.B. (1986). Structure and function of the Ah receptor for 2,3,7,8-tetrachlorodibenzo-*p*-dioxin. Species difference in molecular properties of the receptors from mouse and rat hepatic cytosols. *J. Biol. Chem*. **261**, 3987-3995.

Dressler, K.A., Mathis, S., and Kolensnic, R.M. (1992). Tumor necrosis factor-α activates the sphingomyelin signal transduction pathway in a cell-free system. *Science* **259**, 1769-1771.

Fan, F., Yan, B., Wood, G., Viluksela, M., and Rozman, K.K. (1997). Cytokines (IL-1beta and TNFalpha) in relation to biochemical and immunological effects of 2,3,7,8-tetrachlorodibenzo-*p*-dioxin (TCDD) in rats. *Toxicology* **116,** 9–16.

Febbraio, M., Abumrad, N.A., Hajjar, D.P., Sharma, K., Cheng, W., Pearce, S.F.A., and Silverstein, R.L. (1999). A null mutation in murine CD36 reveals an important role in fatty acid and lipoprotein metabolism. J. Biol. Chem. **274**, 19055–19062.

Fletcher, N., Wahlstrom, D., Lundberg, R., Nilsson, C.B., Nilsson, K.C., Stockling, K., Hellmold, H., and Hakansson, H. (2005). 2,3,7,8-Tetrachlorodibenzo-*p*-dioxin (TCDD) alters the mRNA expression of critical genes associated with cholesterol metabolism, bile acid biosynthesis, and bile transport in rat liver: A microarray study. *Toxicol. Appl. Pharmacol*. **207**, 1-24.

Fujiyoshi, P.T., Michalek, J.E., and Matsumura, F. (2006). Molecular epidemiologic evidence for diabetogenic effects of dioxin exposure in U.S. Air Force veterans of the Vietnam War. *Environ. Health Perspect.* **114**, 1677-83.

Grataroli, R., Boussouar, F., and Benahmed, M. (2000). Role of sphingosine in the tumor necrosis factor α stimulatory effect on lactate dehydrogenase A expression and activity in porcine Sertoli cells. *Biology of Reproduction* **63**, 1473-1481.

Hankinson, O., Brooks, B.A., Weir-Brown, K.I., Hoffman, E.C., Johnson, B.S., Nanthur, J., Reyes, H., and Watson, A.J. (1991). Genetic and molecular analysis of the Ah receptor and Cyp1a1 gene expression. *Biochimie* **73,** 61-66.

Hankinson, O. (1995). The aryl hydrocarbon receptor complex. *Annu. Rev. Pharmacol. Toxicol.* **35**, 307-340.

Hannun, Y.A. (1994). The sphingomyelin cycle and the second messenger function of ceramide. *J. Biol. Chem*. **269**, 3125-3128.

Hannun, Y.A., and Obeid, L.M. (1995). Ceramide: an intracellular signal for apoptosis. *Trends Biochem. Sci.* **20**, 73-77.

Hannun, Y.A. (1996). Functions of ceramide in coordinating cellular responses to stress. *Science* **274**, 1855-1859.

Hushka, L.J., Williams, J.S., and Greenlee, W.F. (1998). Characterization of 2,3,7,8-tetrachlorodibenzofuran-dependent suppression and AH receptor pathway gene expression in the developing mouse mammary gland. *Toxicol. Appl. Pharmacol.* **152**:200–210.

Jahns, G.L., Kent, M.N., Reo, N.V., Burgoon, L.D., Zacharewski, T.R., and DelRaso, N. (2008). Development of Analytical Methods for NMR Spectra and Application to a ^{13}C Toxicology Study. Publication in progress.

Kafafi, S.A., Afeefy, H.Y., Ali, A.H., Said, H.K., and Kafafi, A.G. (1993). Binding of polychlorinated biphenyls to the aryl hydrocarbon receptor. *Environ. Health Perspect*. **101**, 422-428.

Kagan, V.E., Bayir, A., Bayir, H., Stoyanovsky, D., Borisenko, G.G., Tyurina, Y.Y., Wipf, P., Atkinson, J., Greenberger, J.S., Chapkin, R.S., and Belikova, N.A. (2008). Mitochondria-targeted disruptors and inhibitors of cytochrome c/cardiolipin peroxidase complexes: A new strategy in anti-apoptotic drug discovery. *Mol. Nutr. Food Res*.

Kagan, V.E., Tyurina, Y.Y., Bayir, H., Chu, C.T., Kapralov, A.A., Vlasova, I.I., Belikova, N.A., Tyurin, V.A., Amoscato, A., Epperly, M., Greenberger, J., Dekosky, S., Shvedova, A.A., and Jiang, J. (2006). The

"pro-apoptotic genies" get out of mitochondria: oxidative lipidomics and redox activity of cytochrome c/cardiolipin complexes. *Chem. Biol. Interact.* **163(1-2)**, 15-28.

Kagan, V.E., Borisenko, G.G., Tyurina, Y.Y., Tyurin, V.A., Jiang, J., Potapovich, A.I., Kini, V., Amoscato, A.A., and Fujii, Y. (2004). Oxidative lipidomics of apoptosis: redox catalytic interactions of cytochrome c with cardiolipin and phosphatidylserine. *Free Radic. Biol. Med.* **37(12)**, 1963-85.

Katz, L.B., Theobald, H.M., Bookstaff, R.C., and Peterson, R.E. (1984). Characterization of the enhanced paw edema response to carrageenan and dextran in 2,3,7,8-tetrachlorodibenzo-*p*-dioxin-treated rats. *J. Pharmacol.Exp. Ther.* **230,** 670–677.

Kerkvliet, N.I. (1995). Immunological effects of chlorinated dibenzo-*p*-dioxins. *Environ. Health Perspect*. **103,** 47-53.

Kociba, R.J., Keyes, D.G., Beyer, J.E., Carreon, R.M., Wade, C.E., Dittenber, D.A., Kalnins, R.P., Frauson, L.E., Park, C.N., Barnard, S.D., Hummel, R.A., and Humiston, C.G. (1978). Results of a two-year chronic toxicity and oncogenicity study of 2,3,7,8-tetrachlorodibenzo-*p*-dioxin (TCDD) in rats. *Toxicol. Appl. Pharmacol*. **46**, 279-303.

Lee, S.H., Lee, D.Y., Son, W.K., Joo, W.A., and Kim, C.W. (2004). Proteomic characterization of rat liver exposed to 2,3,7,8-tetrachlorobenzo-*p*-dioxin. *J. Proteome Res.* **4**, 335-43.

Le Provost, F., Riedlinger, G., Yim, S.H., Benedict, J., Gonzalez, F.J., Flaws, J., and Henninghausen, L. (2002). The aryl hydrocarbon receptor (AhR) and its nuclear translocator (Arnt) are dispensable for normal mammary gland development but are required for fertility. *Genesis*. **32**, 231–239.

Lucier, G.W., Tritscher, A., Goldsworthy, T., Foley, J., Clark, G., Goldstein, J., and Maronpot, R. (1991). Ovarian hormones enhance 2,3,7,8-tetrachlorodibenzo-*p*-dioxin-mediated increases in cell proliferation and preneoplastic foci in a two-stage model for rat hepatocarcinogenesis. *Cancer Res*. **51**, 1391-1397.

Meneses, P., and Glonek, T. (1988). High resolution ^{31}P NMR of extracted phospholipids. *J. Lipid Res*. **29**, 679-689.

Mattie, M., Brooker, G., and Spiegel, S. (1994). Sphingosine-1-phosphate, a putative second messenger, mobilizes calcium from internal stores via an inositol trisphosphate-independent pathways. *J. Biol. Chem.* **269**, 3181–3188.

Merrill, A.H. (1989) Modulation of protein kinase C and diverse cell functions by sphingosine - a pharmacologically interesting compound linking sphingolipids and signal transduction. *Biochem. Biophys. Acta* **1010**, 131-139.

Merrill, A.H., Jr. (1991). Cell regulation by sphingosine and more complex sphingolipids. *J. Bioenerg. Biomembr.* **23**, 83–104.

Nebert, D.W. (1989). The *Ah* locus: genetic differences in toxicity, cancer, mutation, and birth defects. *CRC Crit. Rev. Toxicol.* **20**, 153-174.

Nebert, D.W., Puga, A., and Vasiliou, V. (1993). Role of the Ah receptor and the dioxin-inducible [*Ah*] gene battery in toxicity, cancer, and signal transduction. *Ann. NY Acad. Sci.* **685,** 624–640.

Nebert, D.W., Roe, A.L, Dieter, M.Z., Solis, W.A., Yang, Y., and Dalton, T.P. (2000). Role of the aromatic hydrocarbon receptor and [Ah] gene battery in the oxidative stress response, cell cycle control, and apoptosis. *Biochem Pharmacol.* **59**, 65-85.

Obeid, L.M., and Hannun, Y.A. (1995). Ceramide: a stress signal and mediator of growth suppression and apoptosis. *J. Cell. Biochem*. **58**, 191-198.

Okey, A.B., Franc, M.A., Moffat, I.D., Tijet, N., Boutros, P.C., Korkalainen, M., Tuomisto, J., and Pohjanvirta, R. (2005). Toxicological implications of polymorphisms in receptors for xenobiotic chemicals: The case of the aryl hydrocarbon receptor. *Toxicol. Appl. Pharmacol.* **207**, 43-51.

Patrick, L. (2002). Nonalcoholic fatty liver disease: relationship to insulin sensitivity and oxidative stress, Treatment approaches using vitamin E, magnesium, and betaine. *Altern Med Rev*. **7**, 276–291.

Pearce, N.J., Yates, J.W., Berkhout, T.A., Jackson, B., Tew, D., Boyd, H., Camilleri, P., Sweeney, P., Gribble, A.D., Shaw, A., and Groot, P.H. (1998). The role of ATP citrate-lyase in the metabolic regulation of plasma lipids. Hypolipidaemic effects of SB-204990, a lactone prodrug of the potent ATP citrate-lyase inhibitor SB-201076. Biochem. J. **334**, 113–119.

Peterfy, M., Phan, J., Xu, P., and Reue, K. (2001). Lipodystrophy in the fld mouse results from mutation of a new gene encoding a nuclear protein, lipin. Nat. Genet. **27**, 121–124.

Petroff, B.K., Gao, X., Rozman, K.K., and Terranova, P.F. (2001). The effects of 2,3,7,8-tetrachlorodibenzo-*p*-dioxin (TCDD) on weight gain and hepatic ethoxyresorufin-o-deethylase (EROD) induction vary with ovarian hormonal status in the immature gonadotropin-primed rat model. *Reprod. Toxicol*. **15**, 269-274.

Pirkle, J.L., Wolfe, W.H., Patterson, D.G., Needham, L.L., Michalek, J.E., Miner, J.C., Peterson, M.R., and Phillips, D.L. (1989). Estimates of the half-life of 2,3,7,8-tetrachlorodibenzo-*p*-dioxin in Vietnam veterans of Operation Ranch Hand. *J. Toxicol. Environ. Health* **27**, 165-171.

Poland, A., Glover, E., and Kende, A.S. (1976). Stereospecific, high affinity binding of 2,3,7,8-tetrachlorodibenzo-*p*-dioxin by hepatic cytosol. Evidence that the binding species is receptor for induction of aryl hydrocarbon hydroxylase. *J. Biol. Chem*. **251**, 4936-4946.

Poland, A., and Knutson, J.C. (1982). 2,3,7,8-tetrachlorodibenzo-*p*-dioxin and related halogenated aromatic hydrocarbons: Examination of the mechanism of toxicity. *Annu. Rev. Pharmacol. Toxicol.* **22,** 517-554.

Puga, A., Maier, A., and Medvedovic, M. (2000). The transcriptional signature of dioxin in human hematoma HepG2 cells. *Biochem. Pharmacol*. **60**, 1129-1142.

Raza, H., Robin, M.A., Fang, J.K., and Avadhani, N.G. (2002). Multiple isoforms of mitochondrial glutathione S-transferases and their differential induction under oxidative stress. *Biochem. J*. **366**, 45–55.

Rose, J.Q., Ramsey, J.C., Wentzler, T.H., Hummel, R.A., and Gehring, P. J. (1976). The fate of 2,3,7,8-tetrachlorodibenzo-*p*-dioxin following single and repeated oral doses to the rat. *Toxicol. Appl. Pharmacol*. **36**, 209–226.

Safe, S. (2001). Molecular biology of the Ah receptor and its role in carcinogenesis. *Toxicol. Lett.* **120**, 1–7.

Schecter, A., Birnbaum, L., Ryan, J.J., and Constable, J.D. (2006). Dioxins: An overview. *Environ Res*. **101**, 419-28.

Senft, A., Dalton, T.P., Nebert, D.W., Genter, M.B., Hutchinson, R.J., and Shertzer, H.G. (2002a). Dioxin increases reactive oxygen production in mouse liver mitochondria. *Toxicol. Appl. Pharmacol*. **178**, 15-21.

Senft, A.P., Dalton, T.P., Nebert, D.W., Genter, M.B. Puga, A., Hutchinson, R.J., Kerzee, J.K., Uno, S., and Shertzer, H.G. (2002b). Mitochondrial reactive oxygen production is dependent on the aromatic hydrocarbon receptor. *Free Radical Biology and Medicine*. **33**, 1268-1278.

Sewall, C.H., Lucier, G.W., Tritscher, A.M., and Clark, G.C. (1993). TCDD-mediated changes in hepatic epidermal growth factor receptor may be a critical event in the hepatocarcinogenic action of TCDD. *Carcinogenesis* **14,** 1885-1893.

Shertzer, H.G., Nebert, D.W., Puga, A., Ary, M., Sonntag, D., Dixon, K., Robinson, L.J., Cianciolo, E., and Dalton, T.P. (1998). Dioxin causes a sustained oxidative stress response in the mouse. *Biochem. Biophys. Res. Commun.* **253**, 44-48.

Sohal, P.S., and Cornell, R.B. (1990). Sphingosine inhibits the activity of rat liver CTP: phosphocholine cytidylyltransferase. *J. Biol. Chem.* **265**, 11746-11750.

Spiegel, S., Olivera, A., and Carlson, R.O. (1993). The role of sphingosine in cell growth regulation and transmembrane signaling. *Adv. Lipid Res.* **25**,105–129.

Spiegel, S., Foster, D., Kolesnick, R. (1996). Signal transduction through lipid second messengers. *Curr. Opin. Cell Biol.* **8**,159–167.

Stohs, S.J., Alsharif, N.Z., Shara, M.A., al Bayati, Z.A., and Wahba, Z.Z. (1989). Evidence for the induction of an oxidative stress in rat hepatic mitochondria by 2,3,7,8-tetrachlorodibenzo-*p*-dioxin (TCDD). *Adv. Exp. Med. Biol.* **283,** 827-831.

Stohs, S.J. (1990). Oxidative stress induced by 2,3,7,8-tetrachlorodibenzo-*p*-dioxin (TCDD). *Free Radical Biol. Med.* **9,** 79-90.

Sullivan, A.C., Triscari, J., Hamilton, J.G., Miller, O.N., and Wheatley, V.R. (1974). Effect of (-)-hydroxycitrate upon the accumulation of lipid in the rat: I. Lipogenesis. *Lipids* **9**, 121–128.

Sun, Y.V., Boverhof, D.R., Burgoon, L.D., Fielden, M.R., and Zacharewski T.R. (2004). Comparative analysis of dioxin response elements in human, mouse, and rat genomic sequences. *Nucleic Acids Res.* **32,** 4512-23.

Sutter, T.R., Guzman, K., Dold, K.M., and Greenlee, W.F. (1991). Targets for dioxin: Genes for plasminogen activator inhibitor-2 and interleukin-1 beta. *Science* **254,** 415–418.

Thurmond, T.S., Silverstone, A.E., Baggs, R.B., Quimby, F.W., Staples, J.E., and Gasiewicz, T.A. (1999). A chimeric aryl hydrocarbon receptor knockout mouse model indicates that aryl hydrocarbon receptor activation in hepatopoietic cells contributes to the hepatic lesions induced by 2,3,7,8-tetrachlorodibenzo-*p*-dioxin. *Toxicol. Appl. Pharmacol*. **158,** 33-40.

Vena, J., Boffetta, P., Becher, H., Benn, T., Bueno-de-Mesquita, H.B., Coggon, D., Colin, D., Flesch-Janys, D., Green, L., Kauppinen, T., Littorin, M., Lynge, E., Matthews, J.D., Neuberger, M., Pearce, N., Pesatori, A.C., Saracci, R., Steenland, K., and Kogevinas, M. (1998). Exposure to dioxin and nonneoplastic mortality in the expanded IARC international cohort study of phenoxy herbicide and chlorophenol production workers and sprayers. *Environ. Health Perspect.* **106**, 645-653.

Vorderstrasse, B.A., Fenton, S.E., Bohn, A.A., Cundiff, J.A., and Lawrence, B.P. (2004). A novel effect of dioxin: exposure during pregnancy severely impairs mammary gland differentiation. *Toxicol. Sci*. **78**, 248–257.

Vos, J.G., Moore, J.A., and Zink, J.G. (1974). Toxicity of 2,3,7,8-tetrachlorodibenzo-*p*-dioxin in C57Bl/6 mice. *Toxicol. Appl. Pharmacol.* **29,** 229-241.

Wahba, Z.Z., Lawson, T.A., and Stohs, S.J. (1988). Induction of hepatic DNA single strand breaks in rats by 2,3,7,8-tetrachlorodibenzo-*p*-dioxin (TCDD). *Cancer Lett.* **29**, 281-286.

Warner, M., Eskenazi, B., Mocarelli, P., Gerthoux, P.M., Samuels, S., Needham, L., Patterson, D., and Brambilla, P. (2002). Serum dioxin concentrations and breast cancer risk in the Seveso Women's Health Study. *Environ. Health Perspect.* **110**, 625–628.

Weinstock, P.H., Bisgaier, C.L., Aalto-Setala, K., Radner, H., Ramakrishnan, R., Levak-Frank, S., Essenburg, A.D., Zechner, R., and Breslow, J.L. (1995). Severe hypertriglyceridemia, reduced high density lipoprotein, and neonatal death in lipoprotein lipase knockout mice. Mild hypertriglyceridemia with impaired very low density lipoprotein clearance in heterozygotes. J. Clin. Invest. **96**, *2555–2568.*

Wettstein M., and Haussinger D. (1997). Cytoprotection by the osmolytes betaine and taurine in ischemia-reoxygenation injury in the perfused rat liver. *Hepatology*. **26**, 1560–1566.

Yagyu, H., Lutz, E.P., Kako, Y., Marks, S., Hu, Y., Choi, S.Y., Bensadoun, A., and Goldberg, I.J. (2002). Very low density lipoprotein (VLDL) receptor-deficient mice have reduced lipoprotein lipase activity. Possible causes of hypertriglyceridemia and reduced body mass with VLDL receptor deficiency. *J. Biol. Chem*. **277**, 10037–10043.

APPENDICES

APPENDIX A – Abbreviations

1,3BPG —— 1, 3-bisphosphoglycerate
ACC —— acetyl-CoA carboxylase
AhR —— aryl hydrocarbon receptor
αKG —— α–ketoglutarate
ANOVA —— analysis of variance
Asp —— aspartate
AST —— aspartate aminotransferase
bHLH-PAS —— basic helix-loop-helix period-aryl hydrocarbon nuclear translocator-single-minded domain
$CDCl_3$ —— deuterchloroform
CDP-Eth —— CDP ethanolamine
$CHCl_3$ —— chloroform
CK —— choline kinase
CoA —— coenzyme A
CPT —— choline phosphotransferase
Cs_2EDTA —— cesium ethylenediaminetetraacetic acid
CsOH —— cesium hydroxide
CYP1A1 —— cytochrome P-450 family 1a1
D_2O —— deuterium oxide
DAG —— diacylglycerol
DAG acyltransferase —— diacylglycerol acyltransferase
DAG kinase —— diacylglycerol kinase
DH —— dehydrogenase
DHAP —— dihydroxyacetone phosphate
EDTA —— ethylenediaminetetraacetic acid
EK —— ethanolamine kinase
EPT —— ethanolamine phosphotransferase
Eth —— ethanolamine
F1,6BP —— fructose-1,6-bisphosphate
F1,6-BPase —— fructose-1,6-bisphosphatase
F6P —— fructose-6-phosphate
FA —— fatty acid
FA acyl-CoA —— fatty acid acyl-coenzyme A
Fasn —— fatty acid synthase
FID —— free induction decay
FR —— fully relaxed
G3P —— glycerol-3-phosphate
G3P-DH —— glycerol-3-phosphate dehydrogenase
G6P —— glucose-6-phosphate
G6Pase —— G6P phosphatase
GA3P-DH —— glyceraldehyde-3-phosphate dehydrogenase
GK —— glucokinase
Glu —— glutamate
GPC —— glycerophosphocholine
GPE —— glycerophosphoethanolamine
GSH —— reduced glutathione
GSSG/GSH —— oxidized to reduced glutathione
HSD ——honestly significant differences
HMG-CoA ——hydroxymethylglutaryl-coenzyme A
i.o. —— immature ovariectomized
LD_{50} —— lethal dose

LDH —— lactate dehydrogenase
LPC —— lysophosphatidylcholine
LSM —— least squares means
Lyso-PA —— lyso-phosphatidic acid
MDH —— malate dehydrogenase
MDPA —— methylenediphosphonic acid
MeOH —— methanol
n —— number of samples
Na_2EDTA —— sodium ethylenediaminetetraacetic acid
NA —— not appropriate
NADH —— reduced nicotinamide adenine dinucleotide
NAD^+ —— nicotinamide adenine dinucleotide
NMR —— nuclear magnetic resonance
NOE —— nuclear overhauser effect
NS —— not significant, no significant difference detected
OAA —— oxaloacetate
OPLS-DA —— orthogonal partial least squares discriminant analysis
PA —— phosphatidic acid
PA phosphohydrolase —— phosphatidic acid phosphohydrolase
PCA —— principal component analysis
PC —— pyruvate carboxylase
Pcho —— phosphocholine
Pcho-CT —— phosphocholine-CDP cytidyltransferase
PDH —— pyruvate dehydrogenase
PEMT —— phosphatidylethanolamine methyltransferase
PEP —— phosphoenolpyruvate
PEPCK —— phosphoenolpyruvate carboxykinase
Peth —— phosphoethanolamine
Peth-CT —— phosphoethanolamine-CDP cytidyltransferase
PFK —— phosphofructokinase
PK —— pyruvate kinase
PLC —— phospholipase-C
PLD —— phospholipase-D
PLA_1,A_2 —— phospholipase-A_1 and A_2
PND —— post-natal day
PS —— partially saturated
PtdC —— phosphatidylcholine
PtdE —— phosphatidylethanolamine
PtdI —— phosphatidylinositol
PtdS —— phosphatidylserine
PtdS-DC —— phosphatidylserine decarboxylase
Pyr —— pyruvate
ROS —— reactive oxygen species
SE —— standard error of the mean
Ser-Eth base exchange —— serine-ethanolamine base exchange
SF —— saturation factor
SphK —— sphingosine kinase
SphM —— sphingomyelin
SphMase —— sphingomyelinase
TAG —— triacylglyceride
TCA —— tricarboxylic acid cycle, Krebs cycle
TCDD —— 2,3,7,8-tetrachlorodibenzo-*p*-dioxin
TNF-α —— tumor necrosis factor-α
TSP —— trimethylsilyl-3-propionic acid sodium salt
TOCSY —— total correlation spectroscopy
TPI —— triose phosphate isomerase

APPENDIX B – Experimental Protocol

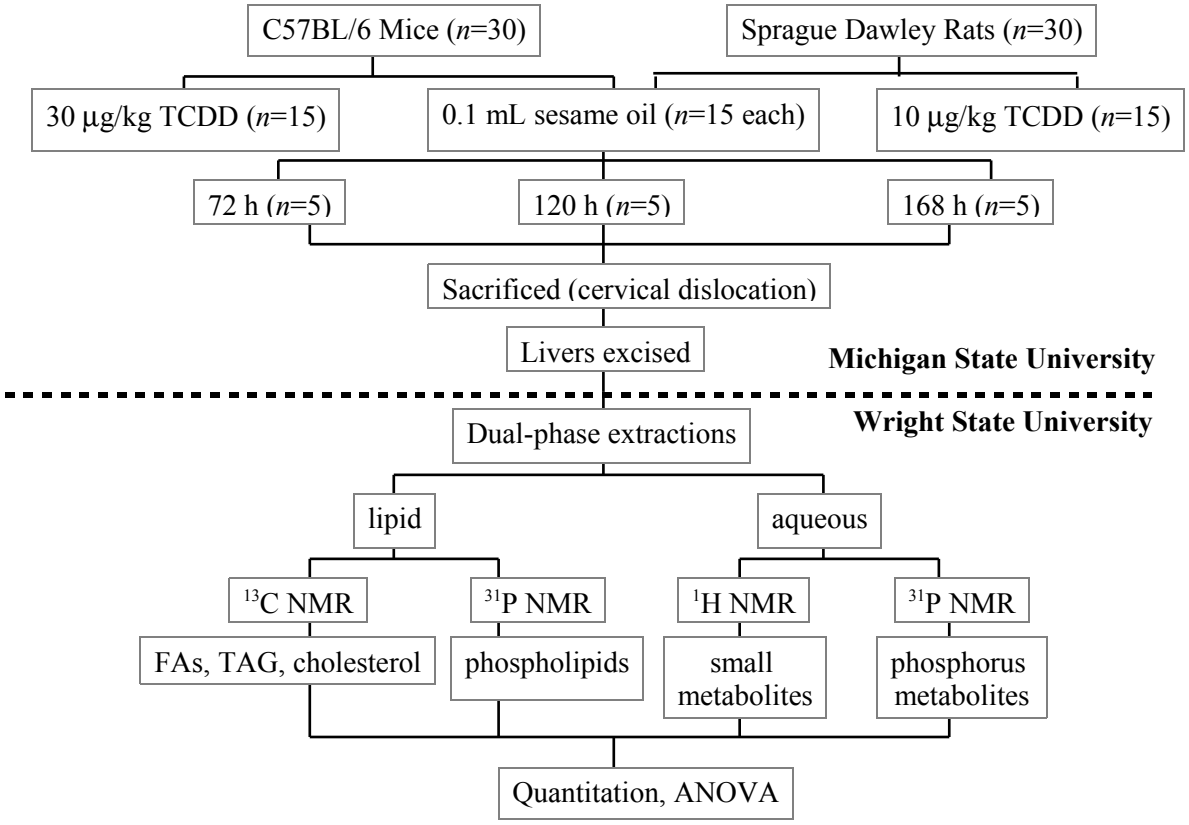

APPENDIX C – QUANTIFICATION

Using cholesterol data

Data Entry:

Volume $CDCl_3$ for sample reconstitution (mL) 0.600
Volume sample transferred to NMR tube (mL) 0.500
Volume Cs_2EDTA soln in NMR tube (mL) 0.200
Change in vol factor for aqs/organic sample 0.355
Final volume in NMR tube (mL) of $CDCl_3$ phase
= Volume of sample transferred to tube + 0.355*Volume of Cs_2EDTA
= 0.5 + 0.355*0.2
= 0.571
Density $CDCl_3$ = 1.500 g/mL
MW of $CDCl_3$ = 120.4
[$CDCl_3$] in NMR tube (mM)
= 1000000*(volume sample transferred to NMR tube*density/ MW)/final volume in tube of $CDCl_3$ phase
=1000000*(0.500*1.500/120.400)/0.571
=10909.345 mM
Tissue weight (g) = 0.499
Intensity of $CDCl_3$ = 100

Saturation Factor:

Under fully relaxed and partially saturated conditions, intensity of $CDCl_3$ = 100
Intensity for cholesterol under:
Fully relaxed (FR) conditions 0.0861734
Partially saturated (PS) conditions 3.18622
equivalent carbons and corrected intensity for cholesterol (CH_3) = 1
Divided the FR and the PS value by 1 = 0.0861734 and 3.18622, respectively
Integral ratio (chol/$CDCl_3$) FR/$CDCl_3$ = FR/100 = 0.00086
PS/$CDCl_3$ = PS/100 = 0.032
SF = FR/PS = 0.027

Let PtdC = Metabolite X

Intensity of Metabolite X = 13.084
equivalent Cs and corrected integral for X = PtdC/1
= 13.084
Intensity ratio measured (X/$CDCl_3$) = intensity of PtdC/intensity of $CDCl_3$
= 13.084/100
= 0.13084
Intensity ratio corrected for saturation (X/$CDCl_3$) = SF*0.13084
= 0.027*0.13084
= 0.0035387
[Metabolite X] in NMR tube (mM) = 0.0035387*[$CDCl_3$] in NMR tube
= 38.6
[Metabolite X] in reconstituted sample (mM)
= 38.6*(final volume in NMR tube of $CDCl_3$ phase/volume sample transferred to tube)
= 38.6 * (0.571/0.500) = 44.09
Metabolite X (μmol) = 44.09*volume $CDCl_3$ for sample reconstitution
= 44.09*0.600
= 26.45
μmol/g tissue = 26.45/tissue weight

= 26.45/0.499
= 53.009472

Let cholesterol = Metabolite X
Intensity of Metab X = 1.23671

equivalent Cs and corrected integral for X = intensity for cholesterol/1
= 1.23671/1
= 1.23671

Intensity Ratio Measured ($X/CDCl_3$) = 1.23671/intensity of $CDCl_3$
= 1.23671/100
= 0.0123671

Intensity Ratio – Corrected for saturation ($X/CDCl_3$) = (0.0123671*SF)
= 0.0123671*0.027
= 0.000334476

[Metab. X] in NMR tube (mM) = 0.000334476*[$CDCl_3$] in NMR tube
= 0.000334476*10909.345
= 3.64891721

[Metab X] in reconstituted sample (mM)
= 3.64891721*(final volume in NMR tube of $CDCl_3$ phase/volume sample transferred to NMR tube)
=3.64891721*(0.571/0.500)
= 4.167063454

Metab. X (μmol) = 4.167063454*volume $CDCl_3$ for sample reconstitution
= 4.167063454*0.600
= 2.500238073

μmol/g tissue = 2.500238073/tissue weight
= 2.500238073/0.499
= 5.01049714

APPENDIX D – Analyses of Variance (ANOVA)